Hodge-deRham Theory of K-Forms on Carpet Type Fractals

Jason Bello[1]
Mathematics Department
UCLA
Los Angeles, CA 90024
jbello01@yahoo.com

Yiran Li and Robert S. Strichartz[2]
Mathematics Department, Malott Hall
Cornell University
Ithaca, NY 14853
yl534@cornell.edu
str@math.cornell.edu

Abstract

We outline a Hodge-deRham theory of K-forms (for k=0,1,2) on two fractals: the Sierpinski Carpet(SC) and a new fractal that we call the Magic Carpet(MC), obtained by a construction similar to that of SC modified by sewing up the edges whenever a square is removed. Our method is to approximate the fractals by a sequence of graphs, use a standard Hodge-deRham theory on each graph, and then pass to the limit. While we are not able to prove the existence of the limits, we give overwhelming experimental evidence of their existence, and we compute approximations to basic objects of the theory, such as eigenvalues and eigenforms of the Laplacian in each dimension, and harmonic 1-forms dual to generators of 1-dimensional homology cycles. On MC we observe a Poincare type duality between the Laplacian on 0-forms and 2-forms. On the other hand, on SC the Laplacian on 2-forms appears to be an operator with continuous (as opposed to discrete) spectrum.

[1]Research supported by the National Science Foundation through the Research Experiences for Undergraduates Program at Cornell.
[2]Research supported by the National Science Foundation, grant DMS - 1162045
2010 *Mathematics Subject Classification*. Primary: 28A80
Keywords and Phrases: Analysis on fractals, Hodge-deRham theory, k-forms, harmonic 1-forms, Sierpinski carpet, magic carpet.

1 Introduction

There have been several approaches to developing an analogue of the Hodge-deRham theory of k-forms on the Sierpinski gasket (SG) and other post-critically finite (pcf) fractals ([ACSY], [C], [CGIS1,2], [CS], [GI1, 2, 3], [H], [IRT]). In this paper we extend the approach in [ACSY] to the Sierpinski carpet (SC) and a related fractal that we call the *magic carpet* (MC). These fractals are not finitely ramified, and this creates technical difficulties in proving that the conjectured theoretical framework is valid. On the other hand, the structure of "2-dimensional" cells intersecting along "1-dimensional" edges allows for a nontrivial theory of 2-forms. Our results are largely experimental, but they lead to a conjectured theory that is more coherent than for SG.

The approach in [ACSY] is to approximate the fractal by graphs, define k-forms and the associated d, δ, Δ operators on them, and then pass to the limit. In the case of SC there is a natural choice of graphs. Figure 1.1 shows the graphs on levels 0, 1, and 2.

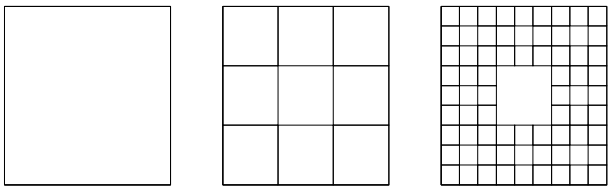

Figure 1.1: The graphs approximating SC on levels 0,1, and 2.

SC is defined by the self-similar identity:

$$SC = \bigcup_{j=1}^{\infty} F_j(SC) \tag{1.1}$$

where F_j is the similarity map of contraction ratio $1/3$ from the unit square to each of the eight of the nine subsquares (all except the center square) after tic-tac-toe subdivision. We define the sequence of graphs

$$\Gamma_m = \bigcup_{j=1}^{\infty} F_j(\Gamma_{m-1}) \tag{1.2}$$

with the appropriate identification of vertices in $F_j(\Gamma_{m-1})$ and $F_k(\Gamma_{m-1})$. Note that a hole in SC on level m does not become visible on the graph until level $m+1$, but it will influence the definition of 2-cells. We denote by $E_0^{(m)}$ the vertices of Γ_m. A 0-form on level m is just a real-valued function $f_0^{(m)}(e_0^{(m)})$ defined on $e_0^{(m)} \in E_0^{(m)}$. We denote the vector space of 0-forms by $\Lambda_0^{(m)}$. The edges $E_1^{(m)}$ of Γ_m exist in opposite orientations $e_1^{(m)}$ and $-e_1^{(m)}$, and a 1-form (element of $\Lambda_1^{(m)}$) is a function on $E_1^{(m)}$ satisfying

$$f_1^{(m)}(-e_1^{(m)}) = -f_1^{(m)}(e_1^{(m)}). \tag{1.3}$$

By convention we take vertical edges oriented upward and horizontal edges oriented to the right. We denote by E_2^m the squares in Γ_m that bound a cell $F_\omega(SC)$, where $\omega = (\omega_1, ..., \omega_m)$ is a word of length m, $\omega_j = 1, 2, ..., 8$ and $F_\omega = F_{\omega_1} \circ F_{\omega_2} \circ ... \circ F_{\omega_m}$. Thus an element e_2^m of E_2^m consists of the subgraph of Γ_m consisting of the four vertices $\{F_\omega(e_0^0) : e_0^0 \in E_0^{(0)}\}$. In particular, there are 8 elements of $E_2^{(1)}$, even thought the central square is a subgraph of the same type. In general $\#E_2^{(m)} = 8^m$, and we will denote squares by the word ω that generates them. A 2-form is defined to be a function $f_2^{(m)}(\omega)$ on $E_2^{(m)}$.

The boundary of a square consists of the four edges in counterclockwise orientation. With our orientation convention the bottom and right edges will have a plus sign and the top and left edges will have minus sign. We build a signum function to do the bookkeeping: if $e_1^{(m)} \subseteq e_2^{(m)}$ then

$$sgn(e_1^{(m)}, e_2^{(m)}) = \begin{cases} +1 & \text{top or right} \\ -1 & \text{bottom or left} \end{cases} \tag{1.4}$$

It is convenient to define $sgn(e_1^{(m)}, e_2^{(m)}) = 0$ if $e_1^{(m)}$ is not a boundary edge of $e_2^{(m)}$. Similarly, if $e_1^{(m)}$ is an edge containing the vertex $e_0^{(m)}$, define

$$sgn(e_0^{(m)}, e_1^{(m)}) = \begin{cases} +1 & e_0^{(m)} \text{ is top or right} \\ -1 & e_0^{(m)} \text{is bottom or left} \end{cases} \tag{1.5}$$

and $sgn(e_0^{(m)}, e_1^{(m)}) = 0$ if $e_0^{(m)}$ is not and endpoint of $e_1^{(m)}$. It is easy to check the consistency condition

$$\sum_{e_1^{(m)} \in E_1^{(m)}} sgn(e_0^{(m)}, e_1^{(m)}) sgn(e_1^{(m)}, e_2^{(m)}) = 0 \tag{1.6}$$

for any fixed $e_0^{(m)}$ and $e_2^{(m)}$, since for $e_0^{(m)} \in e_2^{(m)}$ there are only two nonzero summands, one +1 and the other -1.

We may define the deRham complex

$$0 \to \Lambda_0^{(m)} \xrightarrow{d_0^{(m)}} \Lambda_1^{(m)} \xrightarrow{d_1^{(m)}} \Lambda_2^{(m)} \to 0 \tag{1.7}$$

with the operators

$$d_0^{(m)} f_0^{(m)}(e_1^{(m)}) = \sum_{e_0^{(m)} \in E_0^{(m)}} sgn(e_0^{(m)}, e_1^{(m)}) f_0^{(m)}(e_0^{(m)}) \tag{1.8}$$

(only two nonzero terms) and

$$d_1^{(m)} f_1^{(m)}(e_2^{(m)}) = \sum_{e_1^{(m)} \in E_1^{(m)}} sgn(e_1^{(m)}, e_2^{(m)}) f_1^{(m)}(e_1^{(m)}) \tag{1.9}$$

(only four nonzero terms). The relation

$$d_1^{(m)} \circ d_0^{(m)} \equiv 0 \tag{1.10}$$

is an immediate consequence of (1.6).

To describe the δ operators and the dual deRham complex we need to choose inner products on the spaces $\Lambda_0^{(m)}$, $\Lambda_1^{(m)}$, $\Lambda_2^{(m)}$, or what is the same thing, to choose weights on $E_0^{(m)}$, $E_1^{(m)}$, $E_2^{(m)}$. The most direct choice is to weight each square $e_2^{(m)}$ equally, say

$$\mu_2(e_2^{(m)}) = \frac{1}{8^m}, \tag{1.11}$$

making μ_2 a probability measure on $E_2^{(m)}$. Note that we might decide to renormalize by multiplying by a constant, depending on m, when we examine the question of the limiting behavior as $m \to \infty$. For the weighting on edges we may imagine that each square passes on a quarter of its weight to each boundary edge. Some edges bound one square and some bound two squares, so we choose

$$\mu_1(e_1^{(m)}) = \begin{cases} \dfrac{1}{4 * 8^m} & \text{if } e_1^{(m)} \text{ bounds one square} \\ \dfrac{1}{2 * 8^m} & \text{if } e_1^{(m)} \text{ bounds two squares} \end{cases} \tag{1.12}$$

For vertices we may again imagine the weight of each square being split evenly among its vertices. Now a vertex may belong to 1, 2, 3, or 4 squares, so

$$\mu_0(e_0^{(m)}) = \frac{k}{4 * 8^m} \tag{1.13}$$

if $e_0^{(m)}$ lies in k squares.

The dual deRham complex

$$0 \leftarrow \Lambda_0^{(m)} \xleftarrow{\delta_1^{(m)}} \Lambda_1^{(m)} \xleftarrow{\delta_2^{(m)}} \Lambda_2^{(m)} \leftarrow 0 \tag{1.14}$$

is defined abstractly by $\delta_1^{(m)} = d_0^{(m)*}$ and $\delta_2^{(m)} = d_1^{(m)*}$ where the adjoints are defined in terms of the inner products induced by the weights, or concretely as

$$\delta_1^{(m)} f_1^{(m)}(e_0^{(m)}) = \sum_{e_1^{(m)} \in E_1^{(m)}} \frac{\mu_1(e_1)}{\mu_0(e_0)} sgn(e_0^{(m)}, e_1^{(m)}) f_1^{(m)}(e_1^{(m)}), \tag{1.15}$$

$$\delta_2^{(m)} f_2^{(m)}(e_1^{(m)}) = \sum_{e_2^{(m)} \in E_2^{(m)}} \frac{\mu_2(e_2)}{\mu_1(e_1)} sgn(e_1^{(m)}, e_2^{(m)}) f_2^{(m)}(e_2^{(m)}). \tag{1.16}$$

There are one or two nonzero terms in (1.16) depending on whether $e_1^{(m)}$ bounds one or two squares. In (1.15) there may be 2, 3, or 4 nonzero terms, depending on the number of edges that meet at the vertex $e_0^{(m)}$. The condition

$$\delta_1^{(m)} \circ \delta_2^{(m)} = 0 \tag{1.17}$$

is the dual of (1.10).

We may then define the Laplacian

$$\begin{aligned} -\Delta_0^{(m)} &= \delta_1^{(m)} d_0^{(m)} \\ -\Delta_1^{(m)} &= \delta_2^{(m)} d_1^{(m)} + d_0^{(m)} \delta_1^{(m)} \\ -\Delta_2^{(m)} &= d_1^{(m)} \delta_2^{(m)} \end{aligned} \tag{1.18}$$

as usual. These are nonnegative self-adjoint operators on the associated L^2 spaces, and so have a discrete nonnegative spectrum. We will be examining the spectrum (and associated eigenfunctions) carefully to try to understand what could be said in the limit as $m \to \infty$. Also of particular interest are the harmonic 1-forms $\mathscr{H}_1^{(m)}$, solutions of $-\Delta_1^{(m)} h_1^{(m)} = 0$. As usual theses can be characterized by the two equations

$$d_1^{(m)} h_1^{(m)} = 0 \qquad\qquad \delta_1^{(m)} h_1^{(m)} = 0, \tag{1.19}$$

and can be put into cohomology/homology duality with the homology generating cycles in Γ_m. The Hodge decomposition

$$\Lambda_1^{(m)} = d_0^{(m)} \Lambda_0^{(m)} \oplus \delta_2^{(m)} \Lambda_2^{(m)} \oplus \mathscr{H}_1^{(m)} \tag{1.20}$$

shows that the eigenfunctions of $-\Delta_1^{(m)}$ with $\lambda \neq 0$ are either $d_0^{(m)} f_0^{(m)}$ for $f_0^{(m)}$ an eigenfunction of $-\Delta_0^{(m)}$, or $\delta_2^{(m)} f_2^{(m)}$ for $f_2^{(m)}$ an eigenfunction of $-\Delta_2^{(m)}$ with the same eigenvalue. Thus the nonzero spectrum of $-\Delta_1^{(m)}$ is just the union of the $-\Delta_0^{(m)}$ and $-\Delta_2^{(m)}$ spectrum.

The irregular nature of the adjacency of squares in Γ_m, with the associated variability of the weights in (1.12) and (1.13), leads to a number of complications in the behavior of $-\Delta_2^{(m)}$. To overcome these complications we have invented the fractal MC, that is obtained from SC by making identifications to eliminate boundaries. On the outer boundary of SC we identify the opposite pairs of edges with the same orientation, turning the full square containing SC into a torus. Each time we delete a small square in the construction of SC we identify the opposite edges of the deleted square with the same orientation. We may think of MC as a limit of closed surfaces of genus $g = 1 + (1 + 8 + ... + 8^{m-1})$, because each time we delete and "sew up" we add on a handle to the torus. This surface carries a flat metric with singularities at the corners of each deleted square (all four corners are identified). It is straightforward to see that the limit exists as a metric space. Whether or not the analytic structures (energy, Laplacian, Brownian motion) on SC can be transferred to MC remains to be investigated. Our results give overwhelming evidence that this is the case.

We pass from the graphs Γ_m approximating SC to graphs $\tilde{\Gamma}_m$ approximating MC by making the same identifications of vertices and edges. The graph $\tilde{\Gamma}_1$ is shown in Figure 1.2.

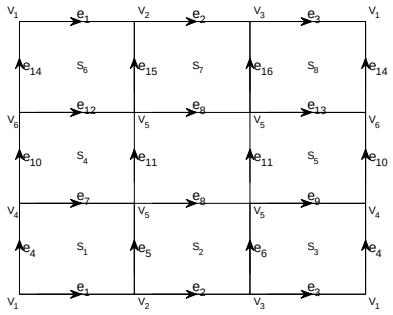

Figure 1.2: $\tilde{\Gamma}_1$ with 6 vertices labeled v_j, 16 edges labeled e_j, and 8 squares labeled s_j.

Each square has exactly 4 neighbors (not necessarily distinct) with each edge separating 2 squares. For example, in Figure 1.2, we see that s_2 has neighbors s_1, s_3, and s_7 twice, as e_2 and e_8 both separate s_2 and s_7. There are two types of vertices, that we call *nonsingular* and *singular*. The nonsingular vertices (all except v_5 in Figure 1.2) belong to exactly 4 distinct squares and 4 distinct edges (two incoming and two outgoing according to our orientation choice). For example, v_1 belongs to squares s_1, s_3, s_6 and s_8 and has incoming edges e_3 and e_{14} and outgoing edges e_1 and e_4. Singular vertices belong to 12 squares (with double counting) and 12 edges (some of which may be loops). In Figure 1.2 there is only one singular vertex v_5. It belongs to squares s_1, s_3, s_6, and s_8 counted once and s_2, s_4, s_5, and s_7 counted twice. In Figure 1.3 we show a neighborhood of this vertex in $\tilde{\Gamma}_2$, with the incident squares and edges shown.

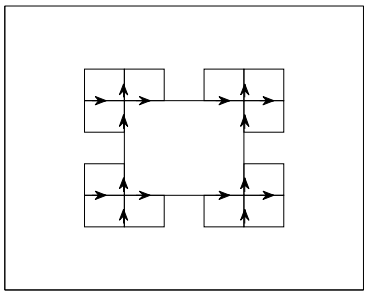

Figure 1.3: A neighborhood in $\tilde{\Gamma}_2$ of vertex v_5 from Figure 1.2.

The definition of the deRham complex for the graphs $\tilde{\Gamma}_m$ approximating MC is exactly the same as for Γ_m approximating SC. The difference is in the dual deRham complex, because the weights are different. We take $\tilde{\mu}_2(e_2^{(m)}) = \dfrac{1}{8^m}$ as before, but now $\tilde{\mu}_1(e_1^{(m)}) = \dfrac{1}{2*8^m}$ because every edge bounds two squares. Finally

$$\tilde{\mu}_0(e_0^{(m)}) = \begin{cases} \dfrac{1}{8^m} & \text{if } e_0^{(m)} \text{ is nonsingular} \\ \dfrac{3}{8^m} & \text{if } e_0^{(m)} \text{ is singular} \end{cases} \tag{1.21}$$

because $e_0^{(m)}$ belongs to 4 squares in the first case and 12 squares in the second case. After that the definitions are the same using the new weights.

Explicitly, we have

$$-\tilde{\Delta}_2^{(m)} f_2^{(m)}(e_2^{(m)}) = 2\Big(\sum_{e_2^{(m)\prime} \sim e_2^{(m)}} f_2^{(m)}(e_2^{(m)}) - f_2^{(m)}(e_2^{(m)\prime})\Big) \tag{1.22}$$

(exactly 4 terms in the sum), the factor 2 coming from $\dfrac{\tilde{\mu}_2(e_2^{(m)})}{\tilde{\mu}_1(e_1^{(m)})}$. Except for the factor 2 this is exactly the graph Laplacian on the 4-regular graph whose vertices are the squares in $\tilde{E}_2^{(m)}$ and whose edge relation is $e_2^{(m)\prime} \sim e_2^{(m)}$ if they have an edge in common (double count if there are two edges in common).

The explicit expression for $-\Delta_0^{(m)}$ is almost as simple:

$$-\tilde{\Delta}_0^{(m)} f_0^{(m)}(e_0^{(m)}) = \begin{cases} \dfrac{1}{2} \displaystyle\sum_{e_0^{(m)\prime} \sim e_0^{(m)}} (f_0^{(m)}(e_0^{(m)}) - f_0^{(m)}(e_0^{(m)\prime})) & \text{if } e_0^{(m)} \text{ is nonsingular} \\ \dfrac{1}{6} \displaystyle\sum_{e_0^{(m)\prime} \sim e_0^{(m)}} (f_0^{(m)}(e_0^{(m)}) - f_0^{(m)}(e_0^{(m)\prime})) & \text{if } e_0^{(m)} \text{ is singular} \end{cases} \tag{1.23}$$

Note that there are 4 summands in the first case and 12 summands in the second case (some may be zero if there is a loop connecting $e_0^{(m)}$ to itself in the singular case). We expect that the spectra of these two Laplacians will be closely related, aside from the multiplicative factor of 4. We may define Hodge star operators from $\Lambda_0^{(m)}$ to $\Lambda_2^{(m)}$ and from $\Lambda_2^{(m)}$ to $\Lambda_0^{(m)}$ by

$$*f_0^{(m)}(e_2^{(m)}) = \frac{1}{4} \sum_{e_0^{(m)} \subseteq e_2^{(m)}} f_0^{(m)}(e_0^{(m)}) \tag{1.24}$$

and

$$*f_2^{(m)}(e_0^{(m)}) = \begin{cases} \dfrac{1}{4} \displaystyle\sum_{e_2^{(m)} \supseteq e_0^{(m)}} f_2^{(m)}(e_2^{(m)}) & \text{if } e_0^{(m)} \text{ is nonsingular} \\ \dfrac{1}{12} \displaystyle\sum_{e_2^{(m)} \supseteq e_0^{(m)}} f_2^{(m)}(e_2^{(m)}) & \text{if } e_0^{(m)} \text{ is singular} \end{cases} \tag{1.25}$$

Note that we do not have the inverse relation that $**$ is equal to the identity in either order. Nor is it true that the star operators conjugate the two Laplacians. However, they are approximately valid,

so we can hope that in the appropriate limit there will be a complete duality between 0-forms and 2-forms with identical Laplacians. Nothing remotely like this valid for SC.

It is also easy to describe explicitly the equations for harmonic 1-forms. The condition $d_1^{(m)} h_1^{(m)}(e_2^{(m)}) = 0$ is simply the condition that the sum of the values $h_1^{(m)}(e_1^{(m)})$ over the four edges of the square is zero (with appropriate signs). Similarly the condition $\delta_1^{(m)} h_1^{(m)}(e_0^{(m)}) = 0$ means the sum over the incoming edges equals the sum over the outgoing edges at $e_0^{(m)}$. Those equations have two redundancies, since the sums $\sum_{e_2^{(m)} \in E_2^{(m)}} d_1^{(m)} f_1^{(m)}(e_2^{(m)})$ and $\sum_{e_0^{(m)} \in E_0^{(m)}} \delta_1^{(m)} f_1^{(m)}(e_0^{(m)})$ are automatically zero for any 1-form $f_1^{(m)}$. Thus in $\tilde{\Lambda}_1^{(1)}$ there is a 4-dimensional space of harmonic 1-forms, and in general the dimension is $2g$, which is exactly the rank of the homology group for a surface of genus g. It is easy to identify the homology generating cycles as the edges that are identified.

The remainder of this paper is organized as follows: In sections 2, 3, 4 we give the results of our computations on SC for 0-forms, 1-forms, and 2-forms. In section 5 we give the results for 0-forms and 2-forms on MC. In section 6 we give the results for 1-forms on MC. We conclude with a discussion in section 7 of all the results and their implications. The website [W] gives much more data than we have been able to include in this paper, and also contains all the programs used to generate the data.

2 0-Forms on the Sierpinski Carpet

The 0-forms on SC will simply be continuous functions on SC, and we can restrict them to the vertices of Γ_m to obtain 0-forms on Γ_m. The Laplacian $-\Delta_0^{(m)}$ is exactly the graph Laplacian of Γ_m with weights on vertices and edges given by (1.12) and (1.13). Thus

$$-\Delta_0^{(m)} f_0^{(m)}(x) = \sum_{y\sim x} c(x,y)(f(x)-f(y)) \tag{2.1}$$

with coefficients show in Figure 2.1

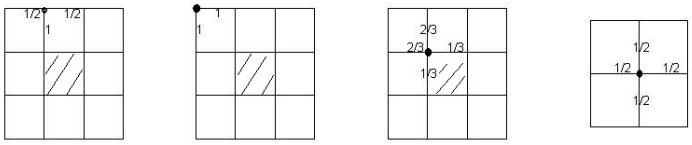

Figure 2.1: Coefficients in (2.1)

The sequence of renormalized Laplacians

$$\{-r^m \Delta_0^{(m)}\} \tag{2.2}$$

for $r \approx 10.01$ converges to the Laplacian on functions ([BB], [KZ], [BBKT] ,[BHS] ,[BKS]).

In Table 2.1 we give the beginning of the spectrum $\{\lambda_j^{(m)}\}$ for $m = 2$, 3, 4 and the ratios $\lambda_j^{(3)}/\lambda_j^{(2)}$ and $\lambda_j^{(4)}/\lambda_j^{(3)}$. The results are in close agreement with the computations in [BHS] and [BKS], and suggest the convergence of (2.2).

m=2	multiplicity	m=3	multiplicity	m=4	multiplicity	$\lambda_j^{(3)}/\lambda_j^{(2)}$	$\lambda_j^{(4)}/\lambda_j^{(3)}$
0.0000	1	0.0000	1	0.0000	1	NaN	NaN
0.0414	2	0.0041	2	0.0004	2	0.1001	0.0999
0.1069	1	0.0109	1	0.0011	1	0.1024	0.1002
0.2006	1	0.0204	1	0.0020	1	0.1017	0.0999
0.2635	2	0.0272	2	0.0027	2	0.1031	0.1002
0.2720	1	0.0284	1	0.0028	1	0.1044	0.1003
0.3927	2	0.0414	2	0.0041	2	0.1053	0.1001
0.4260	1	0.0449	1	0.0045	1	0.1055	0.1002
0.4490	1	0.0472	1	0.0047	1	0.1051	0.1001
0.5276	1	0.0560	1	0.0056	1	0.1062	0.1004
0.6375	2	0.0673	2	0.0067	2	0.1055	0.1002
0.6700	1	0.0696	1	0.0069	1	0.1038	0.0997
0.8405	2	0.0976	2	0.0099	2	0.1161	0.1014
0.8713	1	0.1009	1	0.0102	1	0.1158	0.1008
0.9102	1	0.1069	1	0.0109	1	0.1175	0.1024
0.9336	1	0.1103	1	0.0112	1	0.1181	0.1019

Table 2.1: Eigenvalues of $-\Delta_0^{(m)}$ for $m = 2$, 3, 4 and ratios.

The convergence of (2.2) would imply that $\lim_{m\to\infty} r^m\lambda_j^{(m)} = \lambda_j$ gives the spectrum of the limit Laplacian $-\Delta_0$ on 0-forms on SC. In particular the values $\{r^m\lambda_j^{(m)}\}$ for small values of j (depending on m) would give a reasonable approximation of some lower portion of the spectrum of $-\Delta_0$. To visualize this portion of the spectrum we compute the eigenvalue counting function $N(t) = \#\{\lambda_j \le t\} \approx \#\{r^m\lambda_j^{(m)} \le t\}$ and the Weyl ratio $W(t) = \frac{N(t)}{t^\alpha}$. In Figure we display the graphs of the Weyl ratio using the $m = 1,2,3,4$ approximations, with value α determined from the data to get a function that is approximately constant. As explained in [BKS], we expect $\alpha = \frac{\log 8}{\log r} \approx 0.9026$, which is close to the experimentally determined values. This is explained by the phenomenon called *miniaturization* as described in [BHS]. Every eigenfunction $u_j^{(m)}$ of $\Delta_0^{(m)}$ reappears in miniaturized form $u_k^{(m+1)}$ of $\Delta_0^{(m+1)}$ with the same eigenvalue $\lambda_k^{(m+1)} = \lambda_j^{(m)}$, so in terms of $\Delta_0^{(m)}$ we have $r^{m+1}\lambda_k^{(m+1)} = r(r^m\lambda_j^{(m)})$. We can in fact see this in Table 2.1. In passing from level m to level $m+1$, the number of eigenvalues is multiplied by 8, so we expect to have $N(rt) \approx 8N(t)$, and this explains why $\alpha = \frac{\log 8}{\log r}$ is the predicted power growth factor of $N(t)$. We also expect to see an approximate multiplicative periodicity in $W(t)$, namely $W(rt) \approx W(t)$. It is difficult to observe this in our data, however. We also mention that miniaturization is valid for all k-forms (k =0, 1, 2) on SC and MC. This is most interesting for 0-forms and 2-forms on MC as discussed in Section 5.

In Figure 2.2 we show graphs of selected eigenfunctions on levels 2, 3, 4. We only display those whose eigenspaces have multiplicity one. The convergence is visually evident. To quantify the rate of convergence we give the values of $\|f_j^{(m)}{}_{|_{E_0^{(m-1)}}} - f_j^{(m-1)}\|_2^2$ in Table 2.2. Here the L^2 norm on $E_0^{(m-1)}$ is defined by

$$\|f\|_2^2 = \sum_{e_0^{(m-1)} \in E_0^{(m-1)}} \mu_0(e_0^{(m-1)})|f(e_0^{(m-1)})|^2 \tag{2.3}$$

and we normalize the eigenfunctions so that $\|f_j^{(m-1)}\|_2^2$ and $\|f_j^{(m)}{}_{|_{E_0^{(m-1)}}}\|_2 = 1$. In Figure 2.5 we show the graph of the weyl ratio of eigenvalues of the 0 forms on different levels.

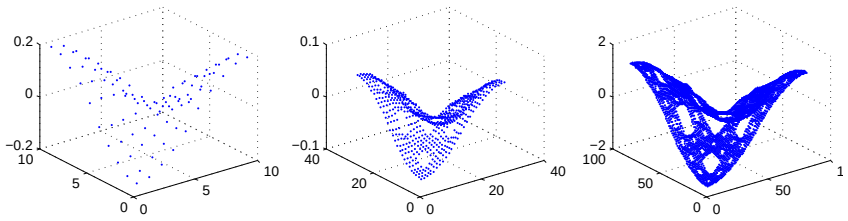

Figure 2.2: graph of eigenfunction of 4th eigenvalue on 0 forms of level 2,3 and 4

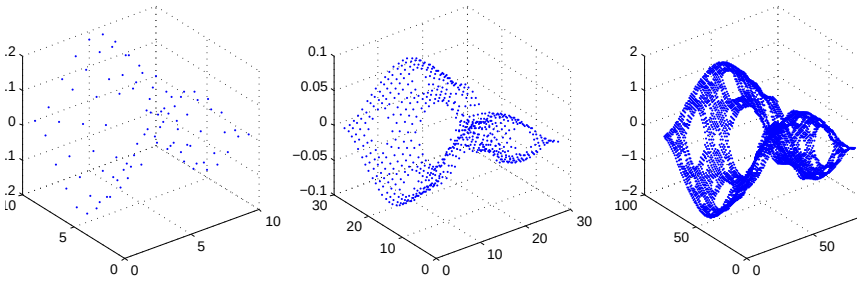

Figure 2.3: graph of eigenfunction of 5th eigenvalue on 0 forms of level 2,3 and 4

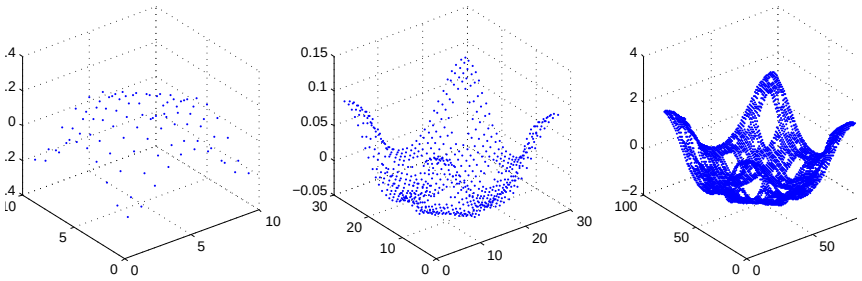

Figure 2.4: graph of eigenfunction of 8th eigenvalue on 0 forms of level 2,3 and 4

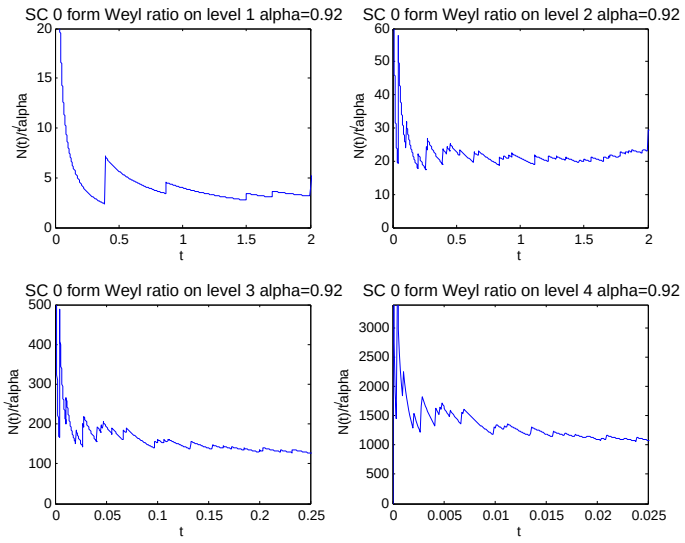

Figure 2.5: graph of eigenfunction of 8th eigenvalue on 0 forms of level 2,3 and 4

# of eigenvalue	Eigenvalue m=2	Eigenvalue m=3	Eigenvalue m=4	level 3 to level2	level 4 to level3
1	0.0000	0.0000	0.0000	0.0000	0.0000
4	0.1069	0.0109	0.0011	0.0001	0.0000
5	0.2006	0.0204	0.0020	0.0006	0.0001
8	0.2720	0.0284	0.0028	0.0003	0.0001
11	0.4260	0.0449	0.0045	0.0009	0.0001
12	0.4490	0.0472	0.0047	0.0013	0.0001
13	0.5276	0.0560	0.0056	0.0025	0.0001
16	0.6700	0.0696	0.0069	0.0161	0.0004
19	0.8713	0.1009	0.0102	0.8818	0.0004
20	0.9102	0.1069	0.0109	0.8755	0.0001
21	0.9336	0.1103	0.0112	0.9226	0.0003

Table 2.2: values of $\|f_j^{(m)}{}_{|_{E_0^{(m-1)}}} - f_j^{(m-1)}\|_2^2$, from level 3 to level 2 and level 4 to level 3 for eigenspaces of multiplicity one

3 1-Forms on the Sierpinski Carpet

The 1-forms on Γ_m are functions on the edges of Γ_m, with $f_1^{(m)}(-e_1^{(m)}) = -f_1^{(m)}(e_1^{(m)})$ if $-e_1^{(m)}$ denotes the edge $e_1^{(m)}$ with opposite orientation. If L denotes any oriented path made up of edges, we may integrate $f_1^{(m)}$ over L by summing:

$$\int_L df_1^{(m)} = \sum_{e_1^{(m)} \subseteq L} f_1^{(m)}(e_1^{(m)}). \tag{3.1}$$

In particular, if $f_1^{(m)} = df_0^{(m)}$ then

$$\int_L df_0^{(m)} = f_0^{(m)}(b) - f_0^{(m)}(a) \tag{3.2}$$

where b and a denote the endpoints of L.

The Hodge decomposition splits this space $\Lambda_1^{(m)}$ of 1-forms into three orthogonal pieces.

$$\Lambda_1^{(m)} = d_0^{(m)}\Lambda_0^{(m)} \oplus \delta_2^{(m)}\Lambda_2^{(m)} \oplus \mathscr{H}_1^{(m)} \tag{3.3}$$

The map $d_0^{(m)} : \Lambda_0^{(m)} \to \Lambda_1^{(m)}$ has the 1-dimensional kernel consisting of constants, and the map $\delta_2^{(m)} : \Lambda_2^{(m)} \to \Lambda_1^{(m)}$ has zero kernel. A dimension count shows

$$dim\mathscr{H}_1^{(m)} = 1 + 8 + ... + 8^{m-1} = \frac{8^m - 1}{7} \tag{3.4}$$

The Laplacian $-\Delta_1^{(m)}$ respects the decomposition, with

$$\begin{aligned} &-\Delta_1^{(m)}(d_0^{(m)} f_0^{(m)}) = d_0^{(m)}(-\Delta_0^{(m)} f_0^{(m)}) = d_0^{(m)}\delta_1^{(m)}(d_0^{(m)} f_0^{(m)}) \\ &-\Delta_1^{(m)}(\delta_2^{(m)} f_2^{(m)}) = \delta_2^{(m)}(-\Delta_2^{(m)} f_1^{(m)}) = \delta_2^{(m)} d_1^{(m)}(\delta_2^{(m)} f_2^{(m)}) \\ &-\Delta_1^{(m)} \mid_{\mathscr{H}_1^{(m)}} = 0 \end{aligned} \tag{3.5}$$

Although we may write $-\Delta_1^{(m)} = d_0^{(m)}\delta_1^{(m)} + \delta_2^{(m)} d_1^{(m)}$, in fact (3.5) is more informative. In particular it shows that the spectrum of $-\Delta_1^{(m)}$ is just a union of the nonzero eigenvalues of $-\Delta_0^{(m)}$ and the eigenvalues of $-\Delta_2^{(m)}$, together with 0 with multiplicity given by (3.4). As such, it has no independent interest, and we will not present a table of its values. Also, when we discuss later the question of renormalizing in order to pass to the limit as $m \to \infty$, we will want to use a different factor for the two terms.

The main object of interest is the space $\mathscr{H}_1^{(m)}$ of harmonic 1-forms. We note that the dimension given by (3.4) is exactly equal to the number of homology generating cycles, one for each square deleted in the construction of SC up to level m. Thus the integrals

$$\int_{\gamma_j} h_1^{(m)} \tag{3.6}$$

as γ_j varies over the cycles and $h_1^{(m)}$ varies over a basis of $\mathscr{H}_1^{(m)}$ give a cohomology/homology pairing.

Conjecture 3.1. *For each m, the matrix (3.6) is invertible.*

If this conjecture is valid (we have verified it for $m \leq 4$) then we may define a canonical basis $h_k^{(m)}$ of $\mathscr{H}_1^{(m)}$ by the conditions

$$\int_{\gamma_j} h_k^{(m)} = \delta_{jk} \tag{3.7}$$

We are particularly interested in the consistency among these harmonic 1-forms as m varies. The cycles at level m contain all the cycles from previous levels and, in addition, the $8^{(m-1)}$ cycles around the level m deleted squares. Thus we can order the cycles consistently from level to level. Also, a 1-from $f_1^{(m)}$ in $\Lambda^{(m)}$ can be restricted to a 1-form in $\Lambda^{(m-1)}$ by defining

$$Rf_1^{(m)}(e_1^{(m-1)}) = \int_{e_1^{(m-1)}} f_1^{(m)}, \tag{3.8}$$

in other words summing the values of $f_1^{(m)}$ on the three level m edges that make up $e_1^{(m-1)}$. Thus we may compare the $\Lambda_1^{(m-1)}$ 1-forms $h_k^{(m-1)}$ and $Rh_k^{(m)}$ for values of k where γ_k is a level $m-1$ cycle. If these are close, we may hope to define a harmonic 1-form on SC by $\lim_{m\to\infty} h_k^{(m)}$. Note that $Rh_k^{(m)}$ will not be a harmonic 1-form in $\mathscr{H}_1^{(m-1)}$. It is easy to see that the equation $d_1^{(m)} h_k^{(m)} = 0$ and the fact that (3.6) is zero for all the level m cycles implies (by addition) $d_1^{(m-1)} Rh_k^{(m)} = 0$. However, there is no reason to believe that $\delta_1^{(m-1)} Rh_k^{(m)}$ should be zero.

In Figure 3.1 to Figure 3.3 we graphically display the numerical data we computed for some of the functions $h_k^{(m)}$ with $k = 1$ and their restrictions. (We rounded the decimal expansions and multiplied by 10^4 so that all values are integers.) The condition $d_1 h_k^{(m)}(e_2^{(m)}) = 0$ says that the sum of $h_k^{(m)}$ on the 4 edges of the square (with appropriate $\pm$ signs) vanishes, or equivalently, the sum on the bottom and right edge equals the sum on top and left edge. A similar condition gives (3.7). The condition $\delta_1 h_k^{(m)}(e_0^{(m)}) = 0$ says that the weighted sum of $h_k^{(m)}$ on the incoming edges at the vertex $e_0^{(m)}$ equals the weighted sum on the outgoing edges, with weights given in Figure 2.1.
To quantify the rate of convergence, we give in Table 3.1 the values of $\|h_k^{(m-1)} - Rh_k^{(m)}\|_2$, where we use an L^2 norm on $E_1^{(m-1)}$.

Another observation is that the size of $h_k^{(m)}$ tends to fall off as the edge moves away from the cycle γ_k as is seen in Figure 3.3. This is not a very rapid decay, however.

Since 1-forms are functions on edges, it appears difficult to display the data graphically. However, there is another point of view, of independent interest, that would enable us to "see" harmonic 1-forms graphically. Note that if $f_0^{(m)}$ is a harmonic function, then $d_0 f_0^{(m)}$ is a harmonic 1-form. This is not interesting globally, since the only harmonic functions are constant. But it is interesting

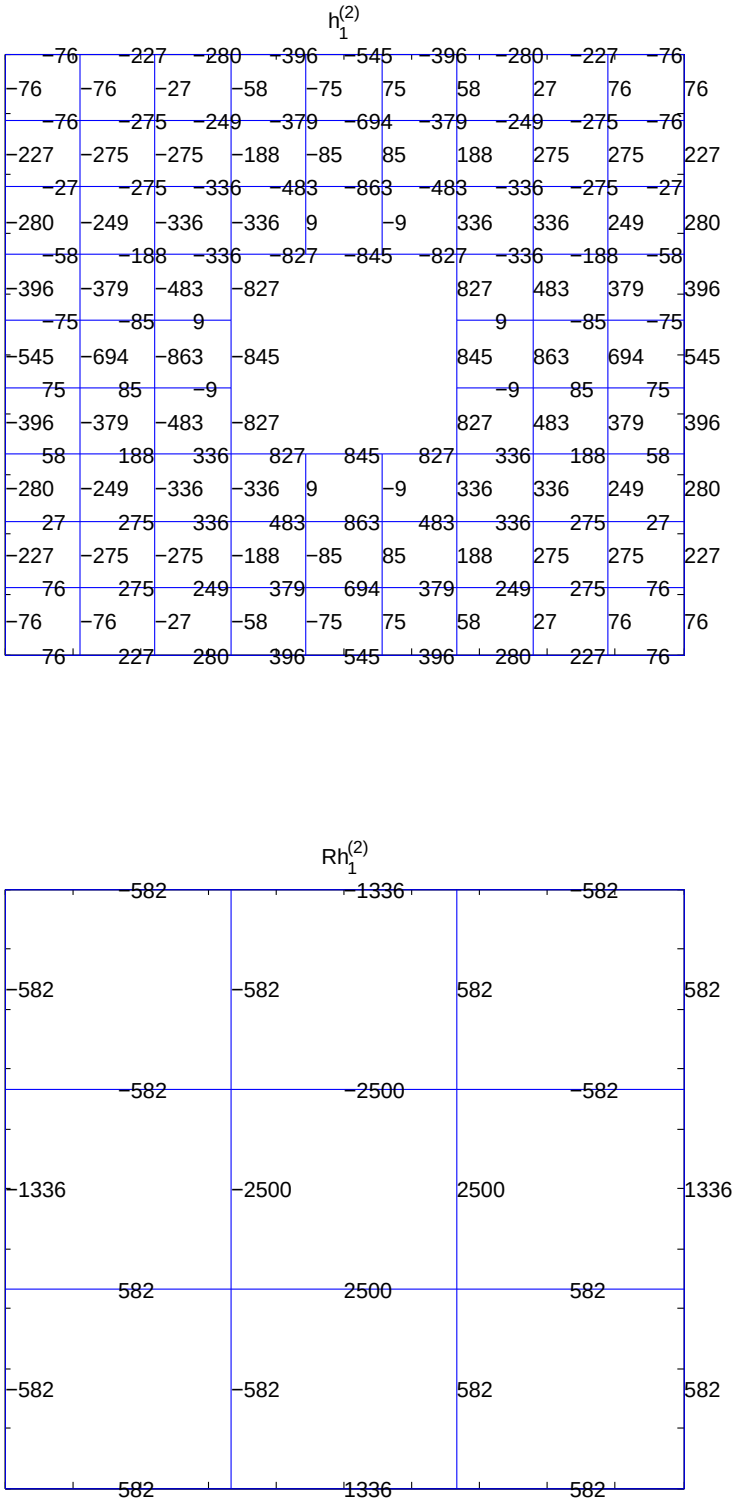

Figure 3.1: values of $h_1^{(2)}$ and the restriction of $h_1^{(2)}$ to $\tilde{E}_1^{(1)}$

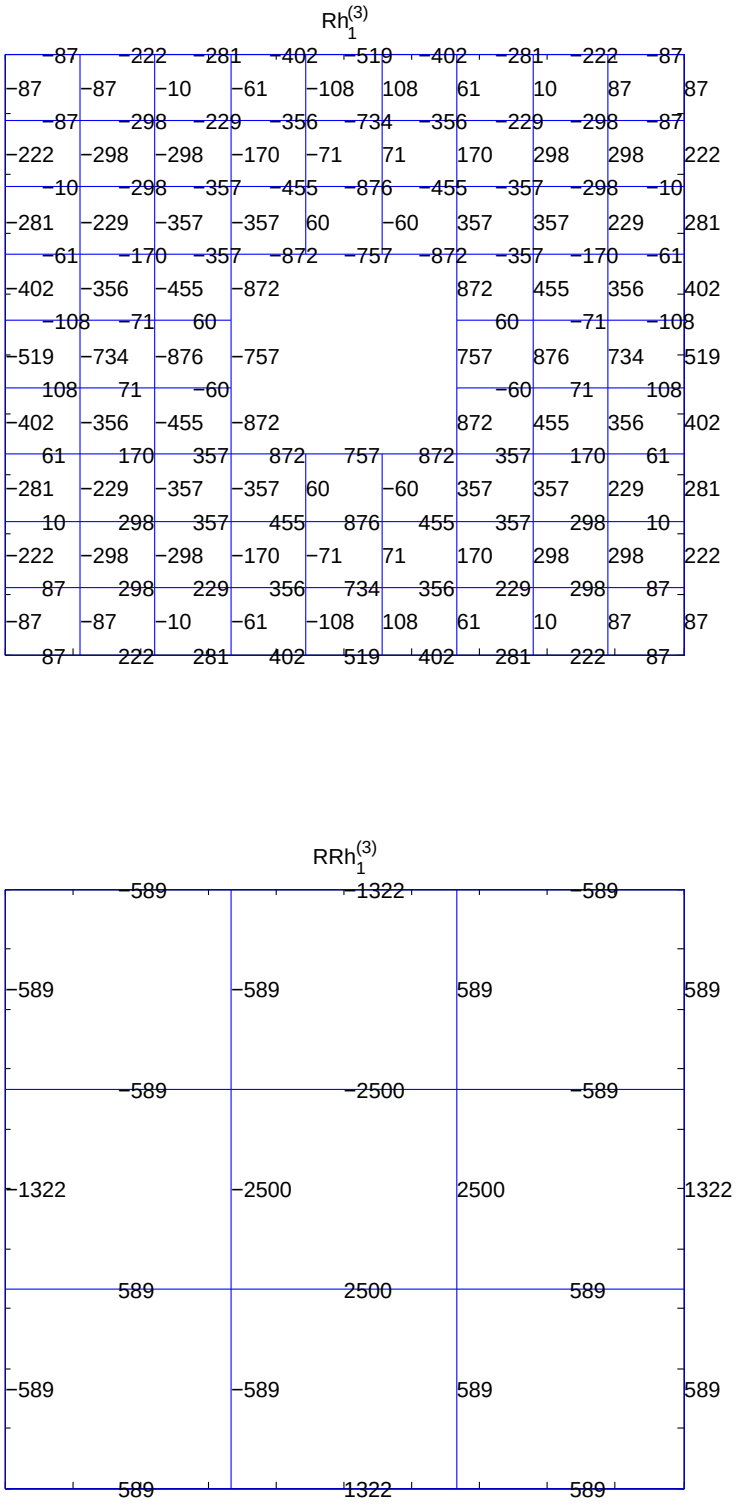

Figure 3.2: values of $Rh_1^{(3)}$ and the restriction of $Rh_1^{(3)}$ to $\tilde{E}_1^{(1)}$

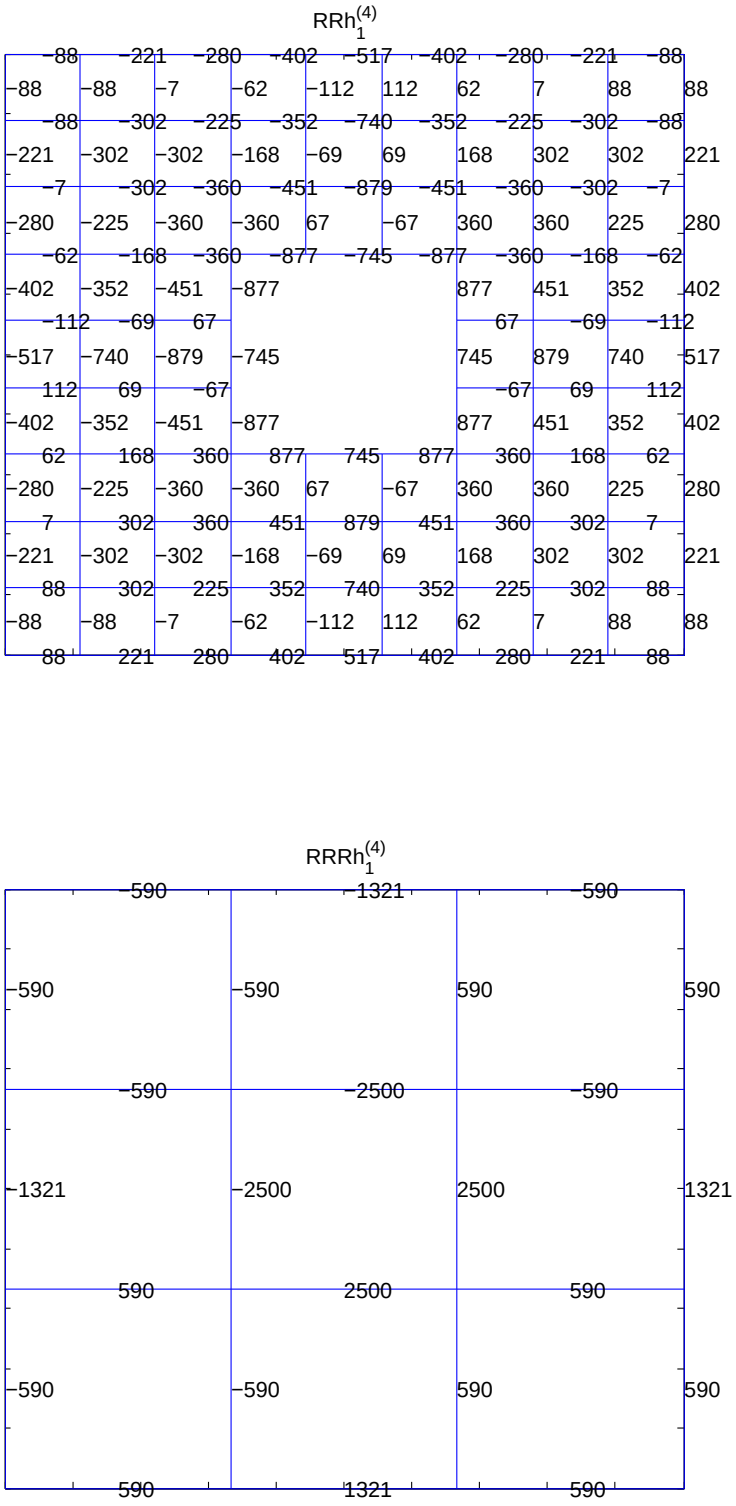

Figure 3.3: values of $RRh_1^{(4)}$ and the restriction of $RRh_1^{(4)}$ to $\tilde{E}_1^{(1)}$

k	$\|\|h^{(2)}_k - Rh^{(1)}_k\|\|$	$\|\|h^{(3)}_k - Rh^{(2)}_k\|\|$	$\|\|h^{(4)}_k - Rh^{(3)}_k\|\|$
1	0.0303	0.0197	0.0140
2		0.0292	0.0206
3		0.0383	0.0224
4		0.0292	0.0206
5		0.0383	0.0224
6		0.0383	0.0224
7		0.0292	0.0206
8		0.0383	0.0224
9		0.0197	0.0206
10			0.0292
11			0.0382
12			0.0343
13			0.0343
14			0.0386
15			0.0343
16			0.0343
17			0.0382
18			0.0292
19			0.0382
20			0.0334

Table 3.1: Values of $\|h_k^{(m-1)} - Rh_k^{(m)}\|_2$

locally, and we can obtain harmonic 1-forms by gluing together 1-forms $d_0 f_0^{(m)}$ for different functions $f_0^{(m)}$ that are locally harmonic. We consider *harmonic mappings* taking values in the circle $\mathbb{R}/\mathbb{Z}$. Such a mapping is represented locally by a harmonic function $f_0^{(m)}$, but when we piece the local representations globally the values may change by an additive integer constant. The additive constant will not change $d_0 f_0^{(m)}$, so this will be a global harmonic 1-form. Again, adding a global constant to $f_0^{(m)}$ will have no effect on $d_0 f_0^{(m)}$. Thus, for each basis element $h_k^{(m)}$ we can construct a harmonic mapping $f_k^{(m)}$ by setting it equal to 0 at the lower left corner of SG, and then integrating using (3.2) to successively extend its values to vertices at the end of an edge where the value at the other endpoint has been determined. For each of the cycles γ_k we can find "cut line" so that the function $f_k^{(m)}$ is single valued away from the cut line, and only satisfies the equation $\delta_1^{(m)} d_0^{(m)} f_k^{(m)}(e_0^{(m)}) = 0$ at the vertices $e_0^{(m)}$ along the cut line if we use different values across the cut line.

Another fundamental question is the behavior of the restriction of a harmonic 1-form to a line segment. Suppose that L is a horizontal or vertical line segment of length one in SC (of course shorter line segments are also of interest, but the answers are expected to be the same). We regard $h_k^{(m)}$ on L as a signed measure on L via (3.1). Do we obtain a measure in the limit as $m \to \infty$? If so, is it absolutely continuous with respect to Lebesgue measure on L? In terms of the restriction of the harmonic mapping $f_k^{(m)}$ to L (we choose L to avoid the cut line), these questions become: is it of bounded variation, and if so is it an absolutely continuous function? Of course we can't answer these questions about the limit, but we can get a good sense by observing the approximations. In Figure 3.4 we graph the restrictions of $h_k^{(m)}$ to L in some cases as m varies. For a quantitative approach to the first question we compute the total variation of the approximations. The results are show in Table 3.2. Note that in this figure and all subsequent graphs of restrictions of 1-forms to lines, we are displaying the graphs of running totals starting at the left end of the interval. Thus in the limit we would hope to get a function of bounded variation (or perhaps even an absolutely continuous function) whose derivative is a measure on the line.

It is more difficult to give quantitative measurements of absolute continuity, so instead we look at the slightly stronger condition that the Radon-Nikodyn derivative belong to L^p for some $p > 1$. If μ is a measure on L and

$$3^{m(p-1)} \sum_{e_1^{(m)} \subseteq L} |\mu(e_1^{(m)})|^p \tag{3.9}$$

is uniformly bounded as $m \to \infty$ for some fixed $p > 1$, then μ is absolutely continuous. In Table 3.3 we give the values of (3.9) for different choices of p for the same harmonic 1-forms considered before.

Of course the same questions are of interest for 1-forms that are eigenfunctions of the Laplacian. In Figures 3.5 and 3.6 and Table 3.4 we give the analogous results for $d_0^{(m)} f_0^{(m)}$ and $\delta_2^{(m)} f_2^{(m)}$ where $f_0^{(m)}$ and $f_2^{(m)}$ are eigenforms for the Laplacians $-\Delta_0^{(m)}$ and $-\Delta_2^{(m)}$.

# of lines \ #of Eigenvalues	1	2	3	4	5	6	7	8	9
1	0.2500	0.4538	0.1457	0.0462	0.6024	0.1062	0.4538	0.1457	0.0462
2	0.2651	0.5175	0.1578	0.0492	0.6202	0.1128	0.5175	0.1578	0.0492
3	0.3104	0.3180	0.1966	0.0587	0.3575	0.1323	0.3180	0.1966	0.0587
4	0.3664	0.2101	0.2588	0.0717	0.2879	0.1570	0.2101	0.2588	0.0717
5	0.0336	0.0716	0.3279	0.0347	0.0206	0.0223	0.0716	0.3279	0.0347
6	0.0336	0.0347	0.3279	0.0716	0.0223	0.0206	0.0347	0.3279	0.0716
7	0.3664	0.0717	0.2588	0.2101	0.1570	0.2879	0.0717	0.2588	0.2101
8	0.3104	0.0587	0.1966	0.3180	0.1323	0.3575	0.0587	0.1966	0.3180
9	0.2651	0.0492	0.1578	0.5175	0.1128	0.6202	0.0492	0.1578	0.5175
10	0.2500	0.0462	0.1457	0.4538	0.1062	0.6024	0.0462	0.1457	0.4538

# of lines \ #of Eigenvalues	1	2	3	4	5	6	7	8	9
1	0.2500	0.4522	0.1442	0.0478	0.6035	0.1082	0.4522	0.1442	0.0478
2	0.2522	0.4616	0.1459	0.0483	0.6059	0.1092	0.4616	0.1459	0.0483
3	0.2590	0.4896	0.1509	0.0496	0.6131	0.1121	0.4896	0.1509	0.0496
4	0.2673	0.5244	0.1574	0.0514	0.6219	0.1158	0.5244	0.1574	0.0514
5	0.1049	0.0805	0.0581	0.0199	0.1124	0.0453	0.0805	0.0581	0.0199
6	0.1180	0.0411	0.0643	0.0223	0.0409	0.0510	0.0411	0.0643	0.0223
7	0.3116	0.3444	0.1937	0.0607	0.4011	0.1352	0.3444	0.1937	0.0607
8	0.3275	0.2885	0.2097	0.0643	0.3528	0.1423	0.2885	0.2097	0.0643
9	0.3512	0.2452	0.2342	0.0696	0.3136	0.1528	0.2452	0.2342	0.0696
10	0.3678	0.2188	0.2582	0.0741	0.2917	0.1603	0.2188	0.2582	0.0741
11	0.0730	0.1184	0.2079	0.0274	0.0198	0.0357	0.1184	0.2079	0.0274
12	0.0568	0.0856	0.2781	0.0300	0.0255	0.0292	0.0856	0.2781	0.0300
13	0.0816	0.0695	0.3578	0.0370	0.0407	0.0369	0.0695	0.3578	0.0370
14	0.0216	0.0131	0.0406	0.0093	0.0103	0.0096	0.0131	0.0406	0.0093
15	0.0216	0.0093	0.0406	0.0131	0.0096	0.0103	0.0093	0.0406	0.0131
16	0.0816	0.0370	0.3578	0.0695	0.0369	0.0407	0.0370	0.3578	0.0695
17	0.0568	0.0300	0.2781	0.0856	0.0292	0.0255	0.0300	0.2781	0.0856
18	0.0730	0.0274	0.2079	0.1184	0.0357	0.0198	0.0274	0.2079	0.1184
19	0.3678	0.0741	0.2582	0.2188	0.1603	0.2917	0.0741	0.2582	0.2188
20	0.3512	0.0696	0.2342	0.2452	0.1528	0.3136	0.0696	0.2342	0.2452
21	0.3275	0.0643	0.2097	0.2885	0.1423	0.3528	0.0643	0.2097	0.2885
22	0.3116	0.0607	0.1937	0.3444	0.1352	0.4011	0.0607	0.1937	0.3444
23	0.1180	0.0223	0.0643	0.0411	0.0510	0.0409	0.0223	0.0643	0.0411
24	0.1049	0.0199	0.0581	0.0805	0.0453	0.1124	0.0199	0.0581	0.0805
25	0.2673	0.0514	0.1574	0.5244	0.1158	0.6219	0.0514	0.1574	0.5244
26	0.2590	0.0496	0.1509	0.4896	0.1121	0.6131	0.0496	0.1509	0.4896
27	0.2522	0.0483	0.1459	0.4616	0.1092	0.6059	0.0483	0.1459	0.4616
28	0.2500	0.0478	0.1442	0.4522	0.1082	0.6035	0.0478	0.1442	0.4522

Table 3.2: Total variation of SC harmonic one forms along horizontal lines at level 2 and level 3

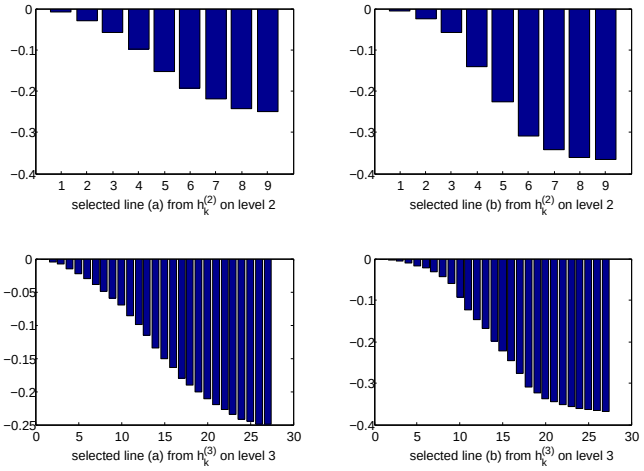
selected line (a) from $h_k^{(2)}$ on level 2
selected line (b) from $h_k^{(2)}$ on level 2
selected line (a) from $h_k^{(3)}$ on level 3
selected line (b) from $h_k^{(3)}$ on level 3

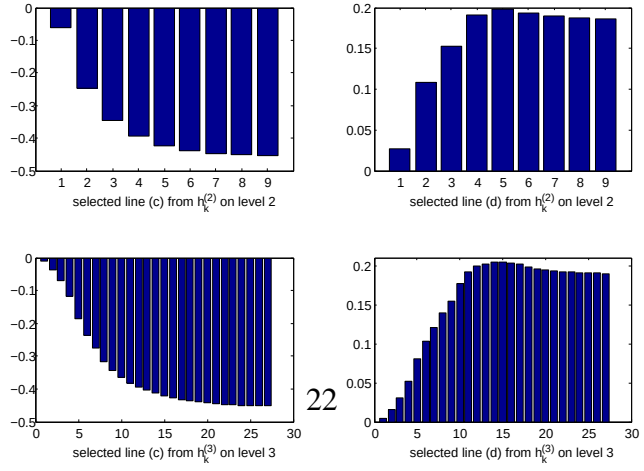
selected line (c) from $h_k^{(2)}$ on level 2
selected line (d) from $h_k^{(2)}$ on level 2
selected line (c) from $h_k^{(3)}$ on level 3
selected line (d) from $h_k^{(3)}$ on level 3

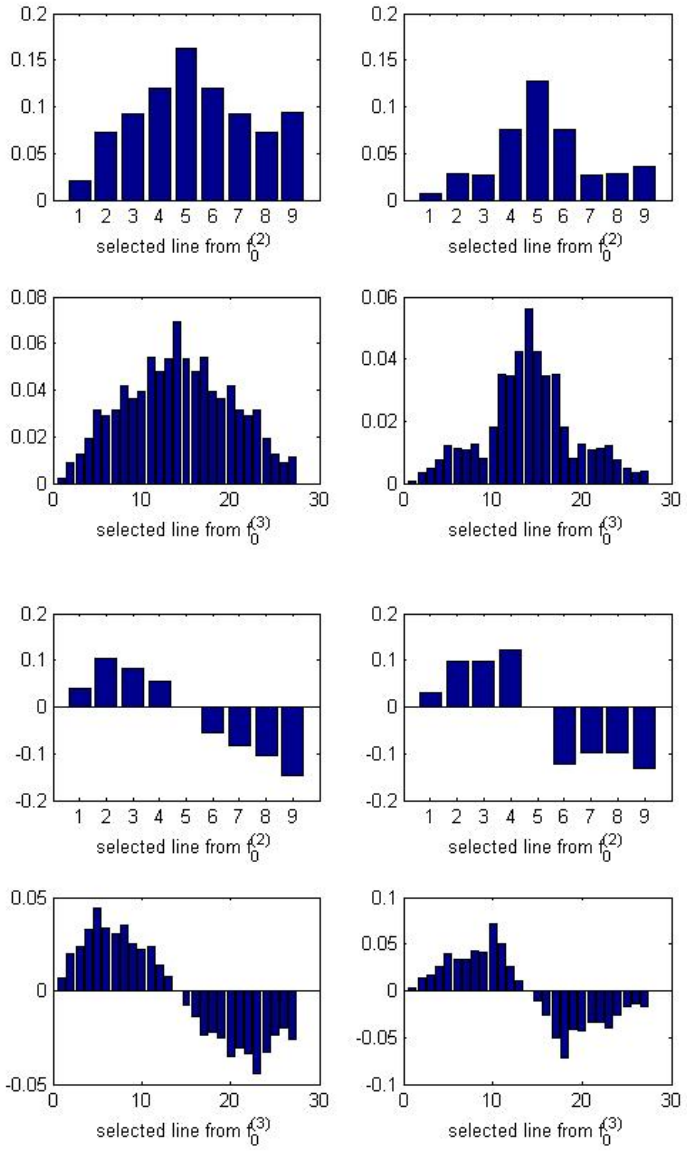

Figure 3.5: restrictions of $d_0^{(m)} f_0^{(m)}$ to L

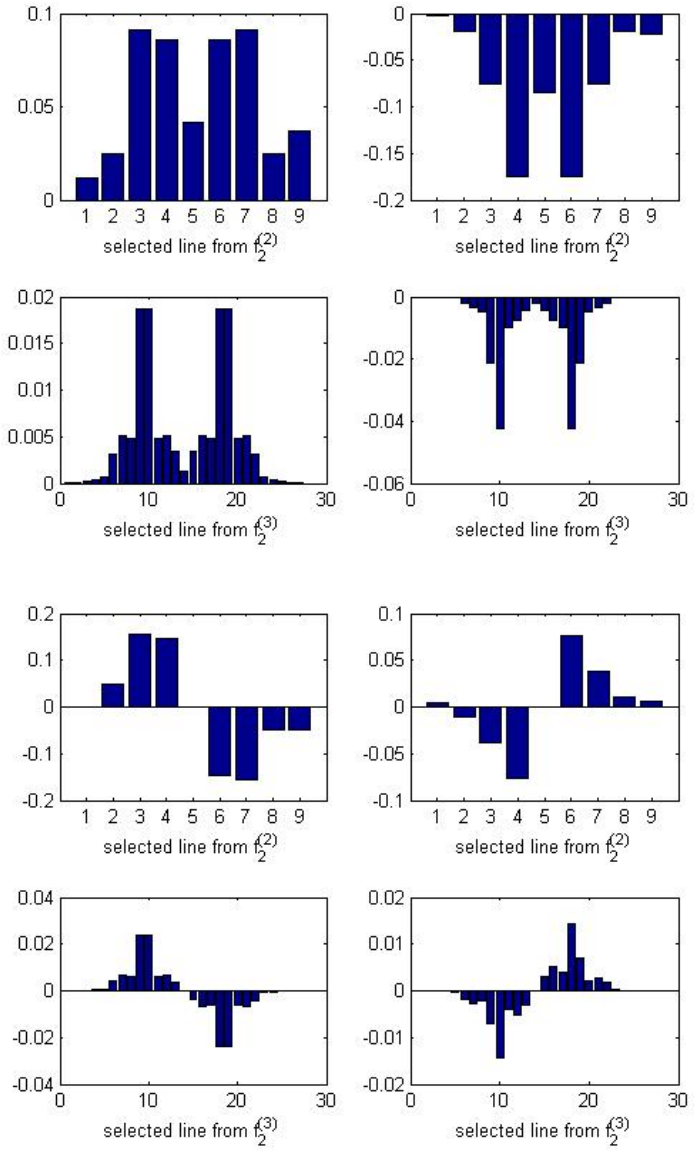

Figure 3.6: restrictions of $\delta_2^{(m)} f_2^{(m)}$ to L

variation sc 1 forms d0 del2.pdf

#of Eigenvalues / # of lines	10	11	12	12	14	15	16	17	18	19
1	0.8041	0.2188	0.7729	0.5680	0.9606	0.5493	0.7267	0.1068	0.8167	0.6692
2	0.8184	0.2302	0.7316	0.5900	0.9189	0.4506	0.6788	0.1634	0.8605	0.6824
3	0.8483	0.2627	0.5853	0.6066	0.7599	0.1986	0.5717	0.1634	0.8605	0.6100
4	0.8718	0.3591	0.4019	0.7008	0.6070	0.2545	0.3988	0.1068	0.8167	0.4781
5	0.1709	0.0878	0.0884	0.3246	0.1296	0.0539	0.2776	0.1089	0.5736	0.1031
6	0.1709	0.0878	0.0884	0.3246	0.1296	0.0539	0.2776	0.1089	0.5736	0.1031
7	0.8718	0.3591	0.4019	0.7008	0.6070	0.2545	0.3988	0.1068	0.8167	0.4781
8	0.8483	0.2627	0.5853	0.6066	0.7599	0.1986	0.5717	0.1634	0.8605	0.6100
9	0.8184	0.2302	0.7316	0.5900	0.9189	0.4506	0.6788	0.1634	0.8605	0.6824
10	0.8041	0.2188	0.7729	0.5680	0.9606	0.5493	0.7267	0.1068	0.8167	0.6692

#of Eigenvalues / # of lines	74	75	76	77	78	79	80	81	82	83
1	0.5240	0.8101	0.8845	0.6348	0.6227	1.0821	0.8203	0.9040	0.6347	0.7826
2	0.5259	0.8131	0.8797	0.6424	0.6114	1.0804	0.8129	0.9201	0.6460	0.7851
3	0.5309	0.8208	0.8617	0.6624	0.5824	1.0682	0.7885	0.9536	0.6696	0.8067
4	0.5372	0.8292	0.8365	0.7002	0.5666	1.0514	0.7581	0.9801	0.6882	0.8026
5	0.2043	0.3101	0.2966	0.2693	0.1679	0.3844	0.2792	0.1921	0.1461	0.1640
6	0.2126	0.3220	0.2596	0.2897	0.1027	0.3636	0.2497	0.1921	0.1461	0.1516
7	0.5646	0.8611	0.6774	0.6747	0.3633	0.8976	0.6912	0.9801	0.6882	0.7291
8	0.5660	0.8686	0.6221	0.7207	0.2651	0.8444	0.6060	0.9536	0.6696	0.6753
9	0.5718	0.8783	0.5310	0.7727	0.2717	0.7743	0.5176	0.9201	0.6460	0.6061
10	0.5807	0.8835	0.4588	0.8178	0.2900	0.7177	0.4484	0.9040	0.6347	0.5454
11	0.1610	0.2259	0.1234	0.4039	0.0905	0.3324	0.3351	0.6134	0.4307	0.1830
12	0.1741	0.1800	0.1495	0.3488	0.0664	0.2100	0.3132	0.6358	0.4464	0.1518
13	0.2489	0.1886	0.2347	0.3241	0.0696	0.1372	0.3040	0.6534	0.4588	0.1998
14	0.0635	0.0490	0.0593	0.0656	0.0138	0.0291	0.0593	0.1281	0.0974	0.0476
15	0.0635	0.0490	0.0593	0.0656	0.0138	0.0291	0.0593	0.1281	0.0974	0.0476
16	0.2489	0.1886	0.2347	0.3241	0.0696	0.1372	0.3040	0.6534	0.4588	0.1998
17	0.1741	0.1800	0.1495	0.3488	0.0664	0.2100	0.3132	0.6358	0.4464	0.1518
18	0.1610	0.2259	0.1234	0.4039	0.0905	0.3324	0.3351	0.6134	0.4307	0.1830
19	0.5807	0.8835	0.4588	0.8178	0.2900	0.7177	0.4484	0.9040	0.6347	0.5454
20	0.5718	0.8783	0.5310	0.7727	0.2717	0.7743	0.5176	0.9201	0.6460	0.6061
21	0.5660	0.8686	0.6221	0.7207	0.2651	0.8444	0.6060	0.9536	0.6696	0.6753
22	0.5646	0.8611	0.6774	0.6747	0.3633	0.8976	0.6912	0.9801	0.6882	0.7291
23	0.2126	0.3220	0.2596	0.2897	0.1027	0.3636	0.2497	0.1921	0.1461	0.1516
24	0.2043	0.3101	0.2966	0.2693	0.1679	0.3844	0.2792	0.1921	0.1461	0.1640
25	0.5372	0.8292	0.8365	0.7002	0.5666	1.0514	0.7581	0.9801	0.6882	0.8026
26	0.5309	0.8208	0.8617	0.6624	0.5824	1.0682	0.7885	0.9536	0.6696	0.8067
27	0.5259	0.8131	0.8797	0.6424	0.6114	1.0804	0.8129	0.9201	0.6460	0.7851
28	0.5240	0.8101	0.8845	0.6348	0.6227	1.0821	0.8203	0.9040	0.6347	0.7826

Table 3.3: Total variation of $d_0^{(m)} f_0^{(m)}$ and $\delta_2^{(m)} f_2^{(m)}$ along horizontal lines at level 2 and level 3

4 2-Forms on the Sierpinski Carpet

In principle, we should think of 2-forms on SC simply as measures. In the Γ_m approximation we have 8^m squares in $E_2^{(m)}$, and our 2-forms $f_2^{(m)}$ assign values to these squares, which may be identified with the m-cells in SC that lie in these squares. It is not clear a priori what class of measures we should consider; the simplest choice is the set of measures absolutely continuous with respect to the standard self-similar measure μ.

The Laplacian $-\Delta_2^{(m)}$ on $\Lambda_2^{(m)}$ is quite different from other Laplacians considered here or elsewhere. In fact, it is the sum of a difference operator and diagonal operator. For a fixed square $e_2^{(m)} \in E_2^{(m)}$ we have

$$d_1^{(m)}\delta_2^{(m)}f_2^{(m)}(e_2^{(m)}) = \sum_{e_1^{(m)}\subseteq e_2^{(m)}} sgn(e_1^{(m)},e_2^{(m)})\delta_2^{(m)}f_2^{(m)}(e_1^{(m)}) \tag{4.1}$$

where the sum is over the four edges of the square. However, $\delta_2^{(m)}f_2^{(m)}(e_2^{(m)})$ depends on the nature of the edge $e_1^{(m)}$, which may bound one or two squares:

$$\delta_2^{(m)}f_2^{(m)}(e_1^{(m)}) = \begin{cases} 4sgn(e_1^{(m)},\tilde{e}_2^{(m)})f_2^{(m)}(\tilde{e}_2^{(m)}) & \text{if } e_1^{(m)} \text{ bounds only } \tilde{e}_2^{(m)} \\ 2\left(sgn(e_1^{(m)},\tilde{e}_2^{(m)})f_2^{(m)}(\tilde{e}_2^{(m)}) + sgn(e_1^{(m)},\tilde{\tilde{e}}_2^{(m)})f_2^{(m)}(\tilde{\tilde{e}}_2^{(m)})\right) & \text{if } e_1^{(m)} \text{ bounds } \tilde{e}_2^{(m)} \text{ and } \tilde{\tilde{e}}_2^{(m)} \end{cases} \tag{4.2}$$

Let $N(e_2^{(m)})$ denote the number of squares adjacent to $e_2^{(m)}$ in Γ_m (2, 3, or 4). Then

$$\begin{aligned} -\Delta_2^{(m)}f_2^{(m)}(e_2^{(m)}) &= d_1^{(m)}\delta_2^{(m)}f_2^{(m)}(e_2^{(m)}) \\ &= 4\left(4-N(e_2^{(m)})\right)f_2^{(m)}(e_2^{(m)}) + 2\sum_{\tilde{e}_2^{(m)}\sim e_2^{(m)}}\left(f_2^{(m)}(e_2^{(m)}) - f_2^{(m)}(\tilde{e}_2^{(m)})\right) \end{aligned} \tag{4.3}$$

Note that

$$-D_2^{(m)}f_2^{(m)}(e_2^{(m)}) = \sum_{\tilde{e}_2^{(m)}\sim e_2^{(m)}}\left(f_2^{(m)}(e_2^{(m)}) - f_2^{(m)}(\tilde{e}_2^{(m)})\right) \tag{4.4}$$

is exactly the graph Laplacian for the cell graph on level m of SC. This Laplacian was first studied in [KZ], and it was proved in [BBKT] that when appropriately normalized it converges to the essentially unique self-similar Laplacian on SC. This was used as the basis for extensive numerical investigations in [BKS]. In other words, if $f_2^{(m)}(e_2^{(m)}) = \int_{e_2^{(m)}} f_0 d\mu$ for some function f_0 in the domain of the Laplacian on SC, then $\lim_{m\to\infty} r^m D_2^{(m)} f_2^{(m)} = c(\Delta f_0)d\mu$ for $r \approx 10.01$.

However, according to (4.3) we have

$$-\Delta_2^{(m)} = M^{(m)} - D_2^{(m)}, \tag{4.5}$$

where $M^{(m)}$ is the operator of multiplication by the function ϕ_m given by

$$\phi_m = 4\left(4 - N(e_2^{(m)})\right) \tag{4.6}$$

Note that ϕ_m takes on values 0, 4, 8. If we were to renormalize $M^{(m)}$ by multiplying by r^m the result would surely diverge. In other words, if there is any hope of obtaining a limit for a class of measures, it would have to be $\lim_{m\to\infty}(-\Delta_2^{(m)})$ without renormalization. Of course the sequence of functions $\{\phi_m\}$ does not converge, so it seems unlikely that we could make sense of $\lim_{m\to\infty}(M^{(m)})$. Thus, although $M^{(m)}$ is clearly the major contributor to the sum (4.5), both operators must play a role if the limit is to exist.

We compute the distribution of the three values of $N(e_2^{(m)})$ as $e_2^{(m)}$ varies over the 8^m squares of level m. Let $n_3^{(m)}$ and $n_4^{(m)}$ denote the number of squares with N value 3 and 4, and $n_{2a}^{(m)}$ and $n_{2b}^{(m)}$ denote the number with $N = 2$, with neighbors on opposite sides ($n_{2a}^{(m)}$) or adjacent sides ($n_{2b}^{(m)}$). In fact $n_{2b}^{(m)} = 4$ since this case only occurs at the four corners of SC. If $e_2^{(m-1)}$ is in one of those cases we may compute the N values on the 8 subsquares as shown in Figure 4.1

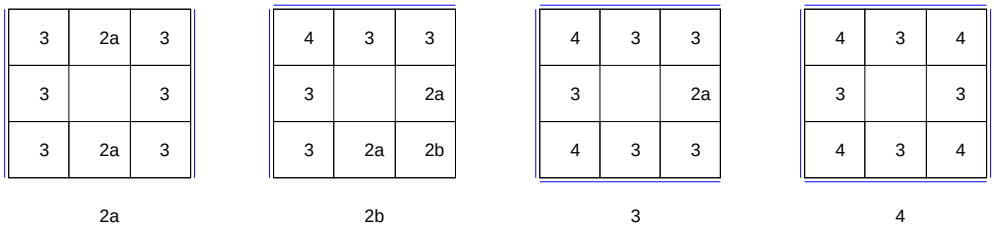

Figure 4.1: Values of N on subsquares. The neighboring edges are marked by a double line.

This gives us the recursion relation

$$\begin{pmatrix} n_{2a}^{(m)} \\ n_{2b}^{(m)} \\ n_3^{(m)} \\ n_4^{(m)} \end{pmatrix} = A \begin{pmatrix} n_{2a}^{(m-1)} \\ n_{2b}^{(m-1)} \\ n_3^{(m-1)} \\ n_4^{(m-1)} \end{pmatrix} \text{ for } A = \begin{pmatrix} 2 & 2 & 1 & 0 \\ 0 & 1 & 0 & 0 \\ 6 & 4 & 5 & 4 \\ 0 & 1 & 2 & 4 \end{pmatrix} \tag{4.7}$$

and so

$$\begin{pmatrix} n_{2a}^{(m)} \\ n_{2b}^{(m)} \\ n_3^{(m)} \\ n_4^{(m)} \end{pmatrix} = A^{m-1} \begin{pmatrix} 4 \\ 4 \\ 0 \\ 0 \end{pmatrix} \tag{4.8}$$

We also note that (1111) is a left eigenvector of A with eigenvalue 8 (in other words column sums are 8), and this implies

$$n_{2a}^{(m)} + n_{2b}^{(m)} + n_3^{(m)} + n_4^{(m)} = 8^m \tag{4.9}$$

as required. We also observe that $\begin{pmatrix} 1 \\ 0 \\ 6 \\ 3 \end{pmatrix}$ is the right eigenvector with eigenvalue 8, so asymptotically

$$\begin{pmatrix} n_{2a}^{(m)} \\ n_{2b}^{(m)} \\ n_3^{(m)} \\ n_4^{(m)} \end{pmatrix} \sim 8^m \begin{pmatrix} .1 \\ 0 \\ .6 \\ .3 \end{pmatrix} \text{ as } m \to \infty. \tag{4.10}$$

Thus the operator $M^{(m)}$ has eigenvalues 0, 4, 8 with multiplicities approximately $\frac{3}{10}8^m$, $\frac{6}{10}8^m$, $\frac{1}{10}8^m$.

The spectrum of the operator $-\Delta_2^{(m)}$ is quite different. Table 4.1 shows the entire spectrum for $m = 1, 2$ and the beginning of the spectrum for $m = 3, 4$.
In Figure 4.2 we give a graphical display of these spectra. In Figure 4.3 we show the graphs of some of the early eigenfuction on levels 2, 3, 4.

The data suggests that there may be a limit

$$-\Delta_2^{(m)} = \lim_{m\to\infty}(-\Delta_2^{(m)}) \tag{4.11}$$

for a class of measures, perhaps $L^2(d\mu)$. The limit operator would be a bounded, self-adjoint operator that is bounded away from zero, hence invertible. The spectrum would be continuous (or a mix of discrete and continuous) with support on a Cantor set.

We can give some explanations as to why we might expect the following types of limits:

$$\delta_1 = \lim_{m\to\infty}\left(\frac{8}{3}\right)^m \delta_2^{(m)} \tag{4.12}$$

$$d_1 = \lim_{m\to\infty}\left(\frac{3}{8}\right)^m d_1^{(m)} \tag{4.13}$$

which are consistent with (4.11). Suppose $f_2 = f d\mu$ for a reasonable function f, and define $f_2^{(m)}(e_2^{(m)}) = \int_{e_2^{(m)}} f d\mu$. Then $f_2^{(m)}(e_2^{(m)})$ is on the order of 8^{-m}. In the definition of $\delta_2^{(m)} f_2^{(m)}$ in (4.2) we note that when $e_1^{(m)}$ bounds only one square, $\delta_2^{(m)} f_2^{(m)}(e_1^{(m)})$ is also on the order of 8^{-m}, so multiplying by $\left(\frac{8}{3}\right)^m$ gives a value on the order of 3^{-m}, which is reasonable for a measure on a line segment L containing $e_1^{(m)}$. On the other hand, if $e_1^{(m)}$ bounds two squares, then the *sgn*

m=1	m=2	m=3	m=4
2.0000	0.9248	0.5101	0.4505
2.2929	0.9497	0.5102	0.4505
2.2929	0.9497	0.5102	0.4505
3.0000	0.9789	0.5104	0.4505
3.0000	1.3068	0.5290	0.4511
3.7071	1.3506	0.5291	0.4511
3.7071	1.3506	0.5291	0.4511
4.0000	1.3989	0.5292	0.4511
	1.5764	0.6251	0.4604
	1.6355	0.6254	0.4604
	1.6355	0.6254	0.4604
	1.7134	0.6257	0.4604
	1.8573	0.6554	0.4614
	1.9559	0.6557	0.4614
	1.9559	0.6557	0.4614
	2.0000	0.6561	0.4614
	2.0593	0.9248	0.5101
	2.0593	0.9280	0.5102
	2.0786	0.9280	0.5102
	2.1187	0.9332	0.5102
	2.1910	0.9395	0.5102
	2.2301	0.9443	0.5102
	2.2929	0.9450	0.5102
	2.2929	0.9450	0.5102
	2.3272	0.9497	0.5102
	2.3272	0.9497	0.5102
	2.3990	0.9527	0.5103
	2.4422	0.9544	0.5103
	2.5000	0.9623	0.5103
	2.5000	0.9690	0.5103
	2.5391	0.9690	0.5103
	2.5391	0.9755	0.5104
	2.6441	0.9789	0.5127
	2.6441	0.9908	0.5127
	2.6673	0.9908	0.5127
	2.7042	1.0021	0.5128
	2.7046	1.0093	0.5139
	2.8809	1.0102	0.5139
	2.8809	1.0102	0.5139
	3.0000	1.0116	0.5139
	3.0000	1.0184	0.5155
	3.0652	1.0247	0.5156
	3.0652	1.0247	0.5156
	3.1920	1.0273	0.5156
	3.2063	1.0350	0.5156
	3.3090	1.0414	0.5157
	3.3173	1.0414	0.5157
	3.3173	1.0500	0.5157
	3.5193	1.0947	0.5197
	3.5193	1.1037	0.5198
	3.5473	1.1037	0.5198
	3.5750	1.1110	0.5198
	3.6632	1.2398	0.5238
	3.6744	1.2400	0.5238
	3.7071	1.2400	0.5238
	3.7071	1.2403	0.5238
	3.7832	1.2717	0.5284
	3.7889	1.2736	0.5284
	3.7889	1.2736	0.5284
	3.8464	1.2761	0.5284
	3.9110	1.3068	0.5290
	3.9671	1.3134	0.5290
	3.9671	1.3134	0.5290
	4.0000	1.3226	0.5290

Table 4.1: Eigenvalues of $-\Delta_2^{(m)}$ for$m$ =1, 2, 3, 4

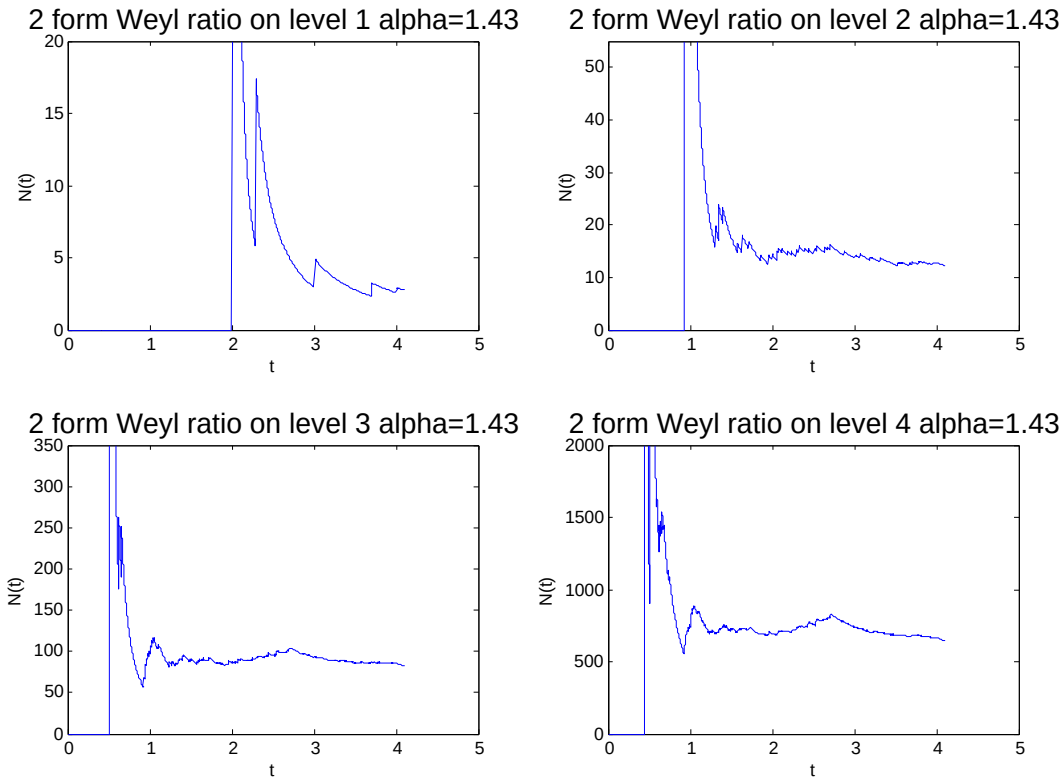

Figure 4.2: Weyl ratio for spectra of SC 2 forms with α=1.43

#	m=2	m=3	m=4	3to2	4to3
1.0000	0.9248	0.5101	0.4505	0.0726	0.0196
4.0000	0.9789	0.5104	0.4505	0.0532	0.0190
5.0000	1.3068	0.5290	0.4511	0.1251	0.0114
8.0000	1.3989	0.5292	0.4511	0.0670	0.0106
9.0000	1.5764	0.6251	0.4604	0.1709	0.0334
12.0000	1.7134	0.6257	0.4604	0.1591	0.0317
13.0000	1.8573	0.6554	0.4614	0.2796	0.0243

Table 4.2: values of $\|f_j^{(m)}{}_{|_{E_2^{(m-1)}}} - f_j^{(m-1)}\|_2^2$, from level 3 to level 2 and level 4 to level 3 for eigenspaces of multiplicity one

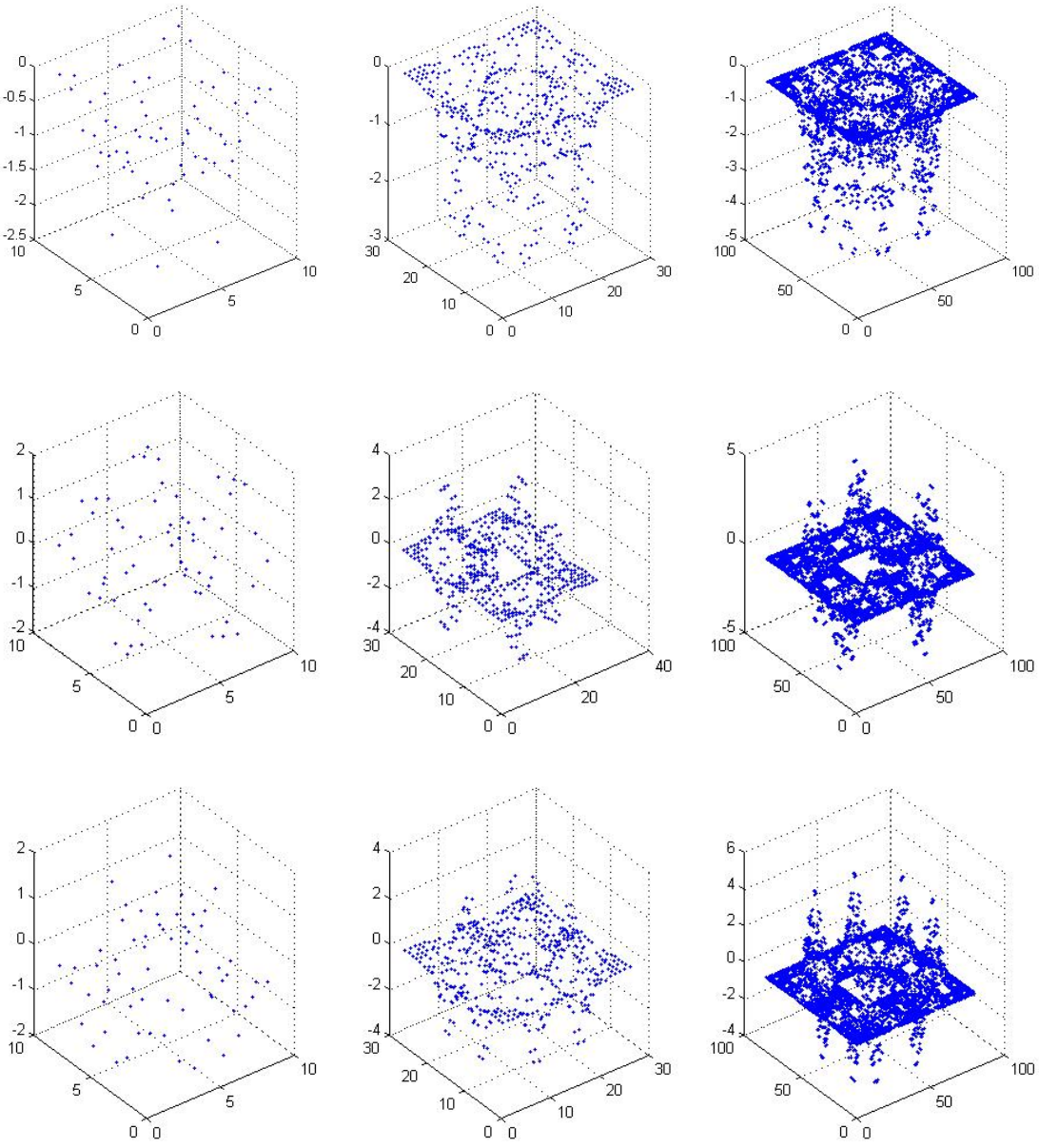

Figure 4.3: graphs of early eigenfunctions of SC 2 forms on level 2, 3, 4

function has opposite signs so $\left(\frac{8}{3}\right)^m \delta_2^{(m)} f_2^{(m)}(e_1^{(m)})$ is close to zero. If we assume the function f is continuous then the limit in (4.12) will give a measure on L equal to $4f|_L dt$ on the portion of L with squares on only one side, and zero on the portion of L with squares on both sides.

Next suppose the f_1 is a measure on each line L in SC that has

$$|f_1(e_1^{(m)})| \leq c3^{-m}. \tag{4.14}$$

Fix a square $e_2^{(m)}$ on level n, and write it as a union of 8^{m-n} squares on level m. We want to define

$$d_1 f_1(e_2^{(n)}) = \lim_{m\to\infty} \left(\frac{3}{8}\right)^m \sum_{e_2^{(m)} \subseteq e_2^{(n)}} d_1^{(m)} f_1^{(m)}(e_2^{(m)}). \tag{4.15}$$

Does this make sense? Because of the cancellation from the *sgn* function on opposite sides of an edge, $\sum_{e_2^{(m)} \subseteq e_2^{(n)}} d_1^{(m)} f_1^{(m)}(e_2^{(m)})$ is just the measure of the boundary of $e_2^{(n)}$ decomposed to level m. This boundary is the union of the 4 edges $e_1^{(n)}$ on the outside of the square, the 4 edges around the inner deleted square on level $n+1$, and in general the $4 * 8^{k-1}$ edges around the 8^k deleted squares on level $n+k$, for $k \leq m-n$.(see Figure 4.4 for $m = n+2$)

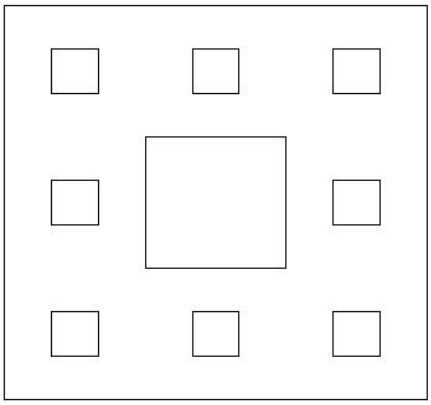

Figure 4.4: Edges in sum for $m = n+2$

Using the estimate (4.14) we have

$$\left|\left(\frac{3}{8}\right)^m \sum_{e_2^{(m)} \subseteq e_2^{(n)}} d_1^{(m)} f_1^{(m)}(e_2^{(m)})\right| \leq 4c\left(\frac{3}{8}\right)^m \left(\frac{1}{3^n} + \frac{8}{3^{n+1}} + \frac{8^2}{3^{n+2}} + \ldots + \frac{8^m}{3^m}\right)$$
$$\leq c.$$

Thus the terms on the right side of (4.15) are uniformly bounded, so it is not unreasonable to hope that the limit exists.

5 0-Forms and 2-Forms on the Magic Carpet

The vertices $\tilde{E}_0^{(m)}$ of $\tilde{\Gamma}_m$ split into singular $\tilde{E}_{0s}^{(m)}$ and nonsingular vertices $\tilde{E}_{0n}^{(m)}$. Let $V_m = \#\tilde{E}_0^{(m)}$, $S_m = \#\tilde{E}_{0s}^{(m)}$, and $N_m = \#\tilde{E}_{0n}^{(m)}$. Then $S_m = 1 + 8 + 8^2 + ... + 8^{m-1} = \dfrac{8^m - 1}{7}$, since each time we remove a square and identify its boundaries we create a single singular vertex. To compute the other two counts, we note that each of the 8^m squares has 4 vertices, and singular vertices arise in 12 different ways, while nonsingular vertices arise in 4 different ways. Thus

$$12S_m + 4N_m = 8^m \tag{5.1}$$

Solving for N_m we obtain $N_m = \dfrac{4 * 8^m + 3}{7}$ and $V_m = \dfrac{5 * 8^m + 2}{7}$. Asymptotically, one-fifth of all vertices are singular.

The Laplacian $-\tilde{\Delta}_0^{(m)}$ given by (1.23) has V_m eigenvalues, starting at $\lambda_0 = 0$ corresponding to the constants. In Table 5.1 we give the beginning of the spectrum for $m = 1, 2, 3, 4$ along with the ratios from levels 3 to 2 and 4 to 3.

We note that the ratios are around $r = 6....$, so we expect

$$-\tilde{\Delta}_0 = \lim_{m\to\infty} r^m \left(-\tilde{\Delta}_0^{(m)}\right) \tag{5.2}$$

to define a Laplacian on MC. At present there is no proof that MC has a Laplacian, so our data is strong experimental evidence that $-\tilde{\Delta}_0$ exists. What is striking is that $r < 8$, in contrast to the factor of ≈ 10.01 for SC. Since the measure renormalization factor is 8^m for both carpets, we conclude that the energy renormalization factor for MC would have to be less than one. In Euclidean spaces or manifolds, this happens in dimensions greater than two. Note that the unrenormalized energy on level m would be

$$\tilde{E}^{(m)}(f_0) = \frac{1}{2 * 8^m} \sum_{e_1^{(m)} \in \tilde{E}_1^{(m)}} |d_0 f_0(e_1^{(m)})|^2, \tag{5.3}$$

so $\widetilde{\mathscr{E}^{(m)}} = r^m \tilde{E}^{(m)}$ means that the graph energy $\displaystyle\sum_{e_1^{(m)} \in \tilde{E}_1^{(m)}} |d_0 f_0(e_1^{(m)})|^2$ is multiplied by $\left(\dfrac{r}{8}\right)^m$ before taking the limit.

In Figure 5.1 we show the graphs of selected eigenfunctions on levels 2, 3, 4. Again we quantify the rate of convergence as in the case of SC by giving in Table 5.2 the values of $\|f_j^{(m)}|_{\tilde{E}_0^{(m-1)}} - f_j^{(m-1)}\|_2^2$.

We give similar data for the spectrum of $-\tilde{\Delta}_2^{(m)}$ defined by (1.22). In order to make the comparison with Table 5.1 clear, we give Table 5.3 the eigenvalues of $-\tilde{\Delta}_2^{(m)}$ multiplied by 0.3221 and ratios. In Table 5.4 we show quantitative rates of convergence. In Figure 5.2 we show graphs of eigenfunctions. In Figure 5.3 we show graphs of $*f_0^{(m)}$ when $f_0^{(m)}$ is an eigenfunction in Figure

λ_1	λ_2	λ_3	λ_4	λ_2/λ_3	λ_3/λ_4
0.0000	0.0000	0.0000	0.0000		
1.5000	0.2877	0.0458	0.0071	6.2809	6.4099
1.7047	0.4458	0.0734	0.0114	6.0699	6.4402
2.5000	0.4458	0.0734	0.0114	6.0699	6.4402
2.5000	0.4496	0.0764	0.0120	5.8860	6.3642
3.1287	0.8333	0.1449	0.0230	5.7521	6.2957
	0.8595	0.1538	0.0244	5.5870	6.2971
	0.8595	0.1538	0.0244	5.5870	6.2971
	0.9862	0.1645	0.0257	5.9938	6.4006
	1.0967	0.1854	0.0289	5.9150	6.4218
	1.1838	0.2175	0.0346	5.4441	6.2913
	1.3014	0.2386	0.0372	5.4555	6.4138
	1.3014	0.2386	0.0372	5.4555	6.4138
	1.5000	0.2684	0.0420	5.5881	6.3862
	1.5000	0.2684	0.0420	5.5881	6.3862
	1.5000	0.2701	0.0428	5.5541	6.3056
	1.5793	0.2849	0.0454	5.5438	6.2771
	1.5793	0.2877	0.0458	5.4898	6.2809
	1.6912	0.3407	0.0552	4.9636	6.1695
	1.7047	0.3869	0.0626	4.4058	6.1772
	1.8770	0.3922	0.0633	4.7861	6.1940
	1.8913	0.3922	0.0633	4.8228	6.1940
	1.9661	0.4169	0.0685	4.7164	6.0849
	1.9661	0.4325	0.0705	4.5462	6.1319

Table 5.1: beginning of the spectrum of $-\tilde{\Delta}_0^{(m)}$ and ratios

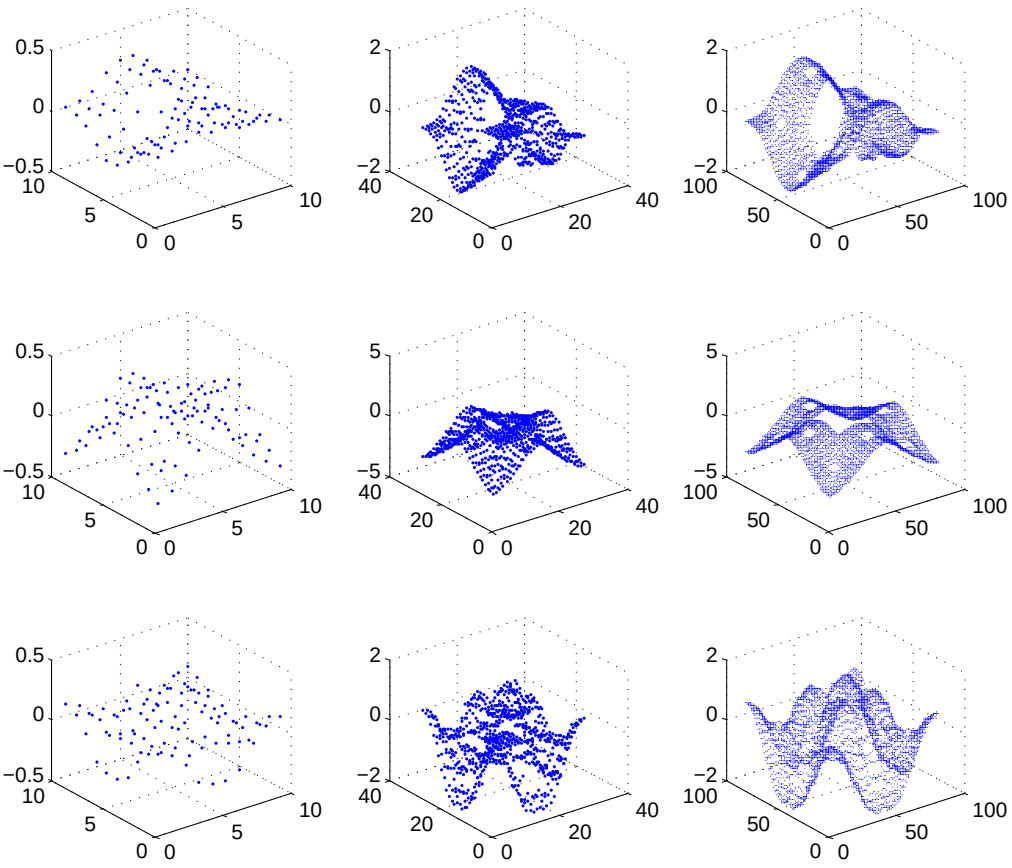

Figure 5.1: graphs of selected eigenfunctions of MC 0 forms on levels 2, 3, 4

#	m=2	m=3	m=4	3to2	4to3
1	0.0000	0.0000	0.0000	0.0000	0.0000
2	0.2877	0.0458	0.0071	0.0000	0.0000
5	0.4496	0.0764	0.0120	0.0001	0.0000
6	0.8333	0.1449	0.0230	0.0002	0.0000
9	0.9862	0.1645	0.0257	0.0004	0.0000
10	1.0967	0.1854	0.0289	0.0008	0.0000
11	1.1838	0.2175	0.0346	0.0008	0.0000
19	1.6912	0.3407	0.0552	0.0004	0.0000
20	1.7047	0.3869	0.0626	0.0435	0.0000
26	2.3156	0.4356	0.0718	0.0435	0.0000
29	2.4459	0.4496	0.1078	0.0435	0.0001
41	3.1105	0.6305	0.1078	0.0435	0.0001
46	3.2194	0.6919	0.1213	0.0435	0.0055

Table 5.2: values of $\|f_j^{(m)}|_{\tilde{E}_0^{(m-1)}} - f_j^{(m-1)}\|_2^2$.

5.1, and in Figure 5.4 we show graphs of $*f_2^{(m)}$ when $f_2^{(m)}$ is an eigenfunction in Figure 5.2. In Figure 5.5 and Figure 5.6, we give the weyl ratios of the eigenvalues of the 0 forms and 2 forms.

Because miniaturization holds we expect a value $\alpha = \frac{\log 8}{\log r} \approx \frac{\log 8}{\log 6}$. We have renormalized the eigenvalues as $\{r^m \lambda_j^{(m)}\}$, with the expectation that in the limit as $m \to \infty$ we obtain eigenvalues of $-\tilde{\Delta}_0$ and $-\tilde{\Delta}_2$ on MC.

m=1	m=2	m=3	m=4	λ_2/λ_3	λ_3/λ_4
-0.0000	-0.0000	0.0000	-0.0000	NaN	NaN
1.2885	0.2841	0.0463	0.0071	6.1409	6.4749
2.1054	0.4449	0.0721	0.0112	6.1710	6.4514
2.1054	0.4449	0.0721	0.0112	6.1710	6.4514
2.5770	0.4889	0.0776	0.0119	6.2970	6.5040
3.8655	0.9193	0.1504	0.0232	6.1139	6.4904
4.3371	0.9553	0.1580	0.0244	6.0455	6.4640
4.3371	0.9553	0.1580	0.0244	6.0455	6.4640
NaN	0.9653	0.1623	0.0253	5.9494	6.4158
NaN	1.0110	0.1792	0.0283	5.6430	6.3393
NaN	1.2077	0.2192	0.0345	5.5097	6.3554
NaN	1.2135	0.2226	0.0356	5.4505	6.2532
NaN	1.2135	0.2226	0.0356	5.4505	6.2532
NaN	1.2885	0.2679	0.0418	4.8091	6.4058
NaN	1.5007	0.2679	0.0418	5.6010	6.4058
NaN	1.5562	0.2699	0.0425	5.7662	6.3573
NaN	1.5562	0.2841	0.0452	5.4771	6.2923
NaN	1.6334	0.2878	0.0463	5.6757	6.2202
NaN	1.7959	0.3541	0.0560	5.0715	6.3241
NaN	1.9528	0.3946	0.0628	4.9493	6.2829
NaN	1.9528	0.3969	0.0630	4.9204	6.3040
NaN	2.0288	0.3969	0.0630	5.1118	6.3040
NaN	2.0840	0.4358	0.0693	4.7825	6.2886
NaN	2.1054	0.4410	0.0712	4.7737	6.1952
NaN	2.1054	0.4410	0.0712	4.7737	6.1952
NaN	2.1700	0.4449	0.0721	4.8774	6.1710
NaN	2.1700	0.4449	0.0721	4.8774	6.1710
NaN	2.3521	0.4529	0.0728	5.1929	6.2232
NaN	2.3579	0.4847	0.0770	4.8648	6.2915
NaN	2.4038	0.4889	0.0776	4.9172	6.2970
NaN	2.4038	0.4971	0.0796	4.8356	6.2415
NaN	2.4760	0.4971	0.0796	4.9807	6.2415
NaN	2.4760	0.5364	0.0870	4.6156	6.1657

Table 5.3: eigenvalues of $-\tilde{\Delta}_2^{(m)}$ multiplied by 0.3221 and ratios

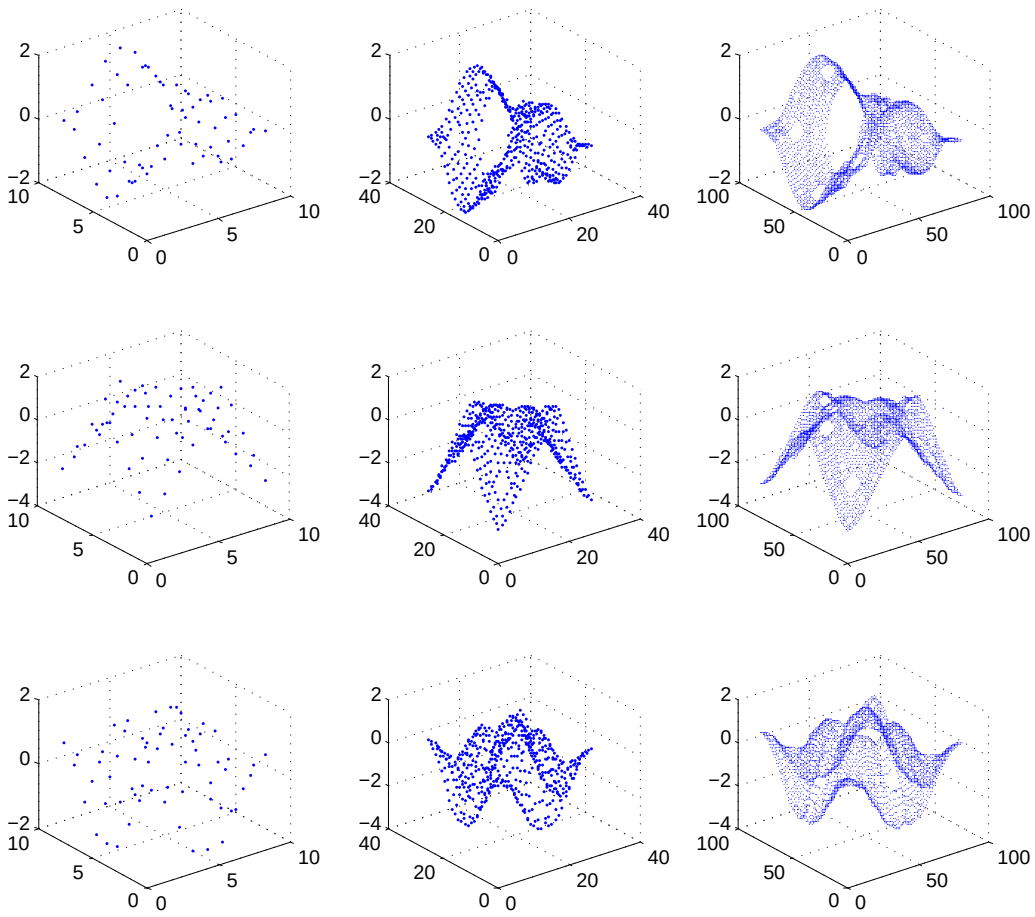

Figure 5.2: graphs of selected eigenfunctions of MC 2 forms on levels 2, 3, 4

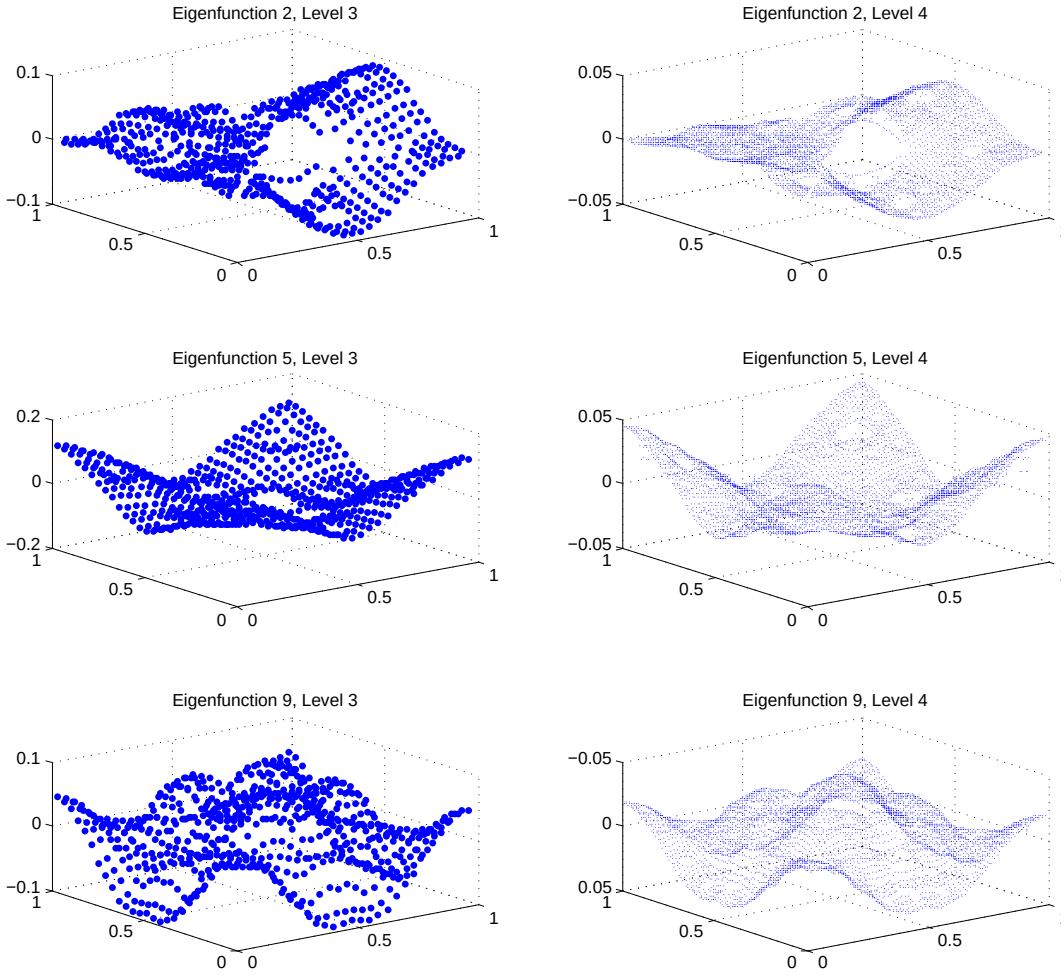

Figure 5.3: graphs of $*f_0^{(m)}$ when $f_0^{(m)}$ is an eigenfunction in Figure 5.1

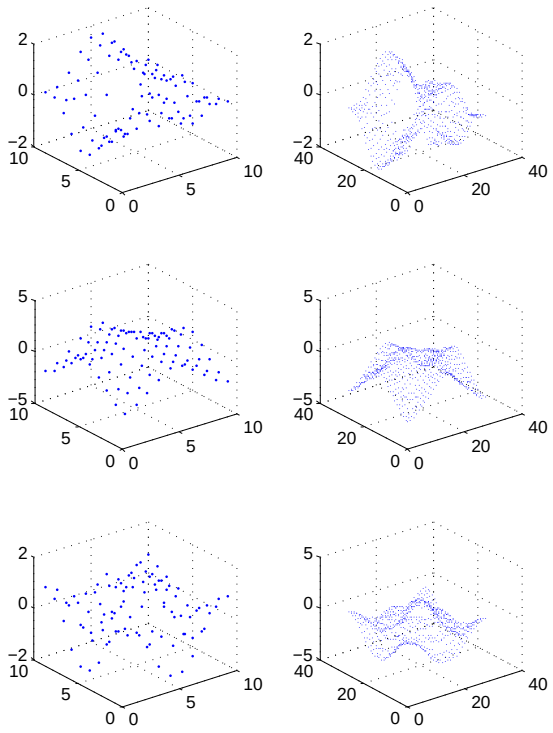

Figure 5.4: graphs of $*f_2^{(m)}$ when $f_2^{(m)}$ is an eigenfunction in Figure 5.2

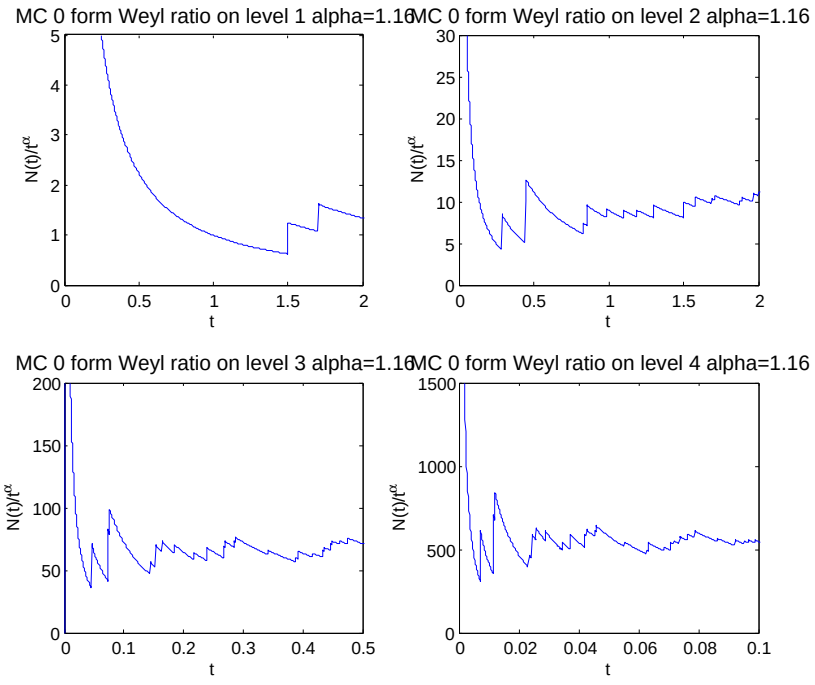

Figure 5.5: Weyl ratio of MC 0 forms eigenvalues

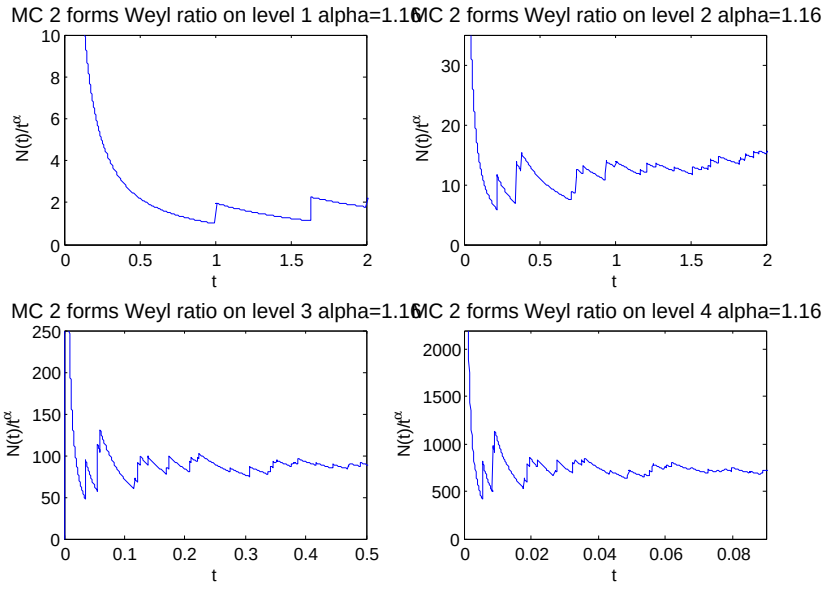

Figure 5.6: Weyl ratio of MC 2 forms eigenvalues

#	m=2	m=3	m=4	3to2	4to3
1	0	0	0	0	0
2	0.2205	0.0359	0.0055	0.0006	0.0001
5	0.3794	0.0602	0.0093	0.0012	0.0002
6	0.7135	0.1167	0.0180	0.0051	0.0003
9	0.7492	0.1259	0.0196	0.0056	0.0004
10	0.7846	0.1391	0.0219	0.0018	0.0004
11	0.9373	0.1701	0.0268	0.0350	0.0011

Table 5.4: values of $\|f_j^{(m)}|_{\hat{E}_2^{(m-1)}} - f_j^{(m-1)}\|_2^2$

6 1-Forms on the Magic Carpet

We indicate briefly how the theory differs from SC. We have the analogs of (3.1), (3.2) and (3.3), but the dimension count is different because $\tilde{\delta}_2^{(m)}$ also has a 1-dimensional kernel, namely the constants. There are exactly $2*8^m$ edges, since each edge is the boundary of exactly two squares, so

$$dim\mathscr{H}_1^{(m)} = 2*8^m - 8^m - \frac{5*8^m+1}{7} + 2 = \frac{2*8^m+12}{7}. \tag{6.1}$$

On the other hand, the surface approximating MC on level m has genus $g = \dfrac{8^m+6}{7}$, and the cycles generating the homology are in one-to-one correspondence with the horizontal and vertical identified edges. The analog of Conjecture 3.1 is true, in fact it is a well-known result in topology.

In Figure 6.1 to Figure 6.3 we show the values of $h_1^{(2)}$, $h_1^{(3)}$ and the restriction of $h_1^{(3)}$ to $\tilde{E}_1^{(2)}$ where γ_1 is the top and bottom horizontal line. There are some surprising features of these 1-forms that may be explained by symmetry. Let R_H denote the horizontal reflection and R_V the vertical reflection about the center. Note that $R_H\gamma_1 = -\gamma_1$ because the orientation is reversed, while $R_V\gamma_1 = \gamma_1$. Since $-h_1^{(m)}(R_Hx)$ and $h_1^{(m)}(R_Vx)$ are harmonic 1-forms with the same integrals around cycles as $h_1^{(m)}$, it follows by uniqueness that $-h_1^{(m)}(R_Hx) = h_1^{(m)}(x)$ and $h_1^{(m)}(R_Vx) = h_1^{(m)}(x)$. This implies that $h_1^{(m)}$ vanishes identically along the cycle consisting of the vertical edges of the large square, and indeed any square that is symmetric with respect to R_H. Certain other vanishings of $h_1^{(m)}$ are accidental to the level m, and do not persist when m increases. For example, every cycle of level m contains just a single edge, so vanishing of the integral forces vanishing on the edge. Sometimes this has a ripple effect. For example, consider the region in the top center of the level 2 graph show in Figure 6.4, where the horizontal symmetry has been used in labeling edges. We obtain the equation $2a+b=0$ from the equation $\tilde{d}_1^{(2)}\tilde{h}_1^{(2)} = 0$ on the small square, and the equation $2c+b=0$ from $\int_\gamma \tilde{h}_1^{(2)} = 0$ on the cycle along the top of the big square. Finally the equation $a+c-b=0$ comes from $\tilde{\delta}_1^{(2)}\tilde{h}_1^{(2)} = 0$ at the indicated point. These yield $a=b=c=0$ that we see in Figure 6.1 to Figure 6.3.

If γ_2 denote the cycle along the vertical edges of lines bounding MC, then $h_2^{(m)}$ is just a rotation of $h_1^{(m)}$. So the next interesting cycle γ_3 is the top and bottom identified lines around the center deleted square on level 1. In Figure 6.5 we show $h_3^{(2)}$, $h_3^{(3)}$ and the restriction of $h_3^{(3)}$ to $\tilde{E}_1^{(2)}$. The website [] has many more similar illustrations of other harmonic 1-forms.

To quantify the rate of convergence we give in Table 6.1 the values of $\|h_k^{(m)} - Rh_k^{(m)}\|_2$ analogous to Table 3.1.

As in the case of SC, we investigate the behavior of restrictions of 1-forms to line segments. In Figure 6.5 we graph the restrictions of some $h_k^{(m)}$, analogous to Figure 3.4. In Table 6.2 we compute total variations of approximations, analogous to Table 3.2. Table 6.3, analogous to Table 3.3, shows the values of (3.9) for different values of p. In Figure 6.6 and Figure 6.7 and Table 6.4 we give analogous results for $\tilde{d}_0^{(m)}f_0^{(m)}$ and $\tilde{\delta}_2^{(m)}f_2^{(m)}$ where $f_0^{(m)}$ and $f_2^{(m)}$ are eigenforms of the

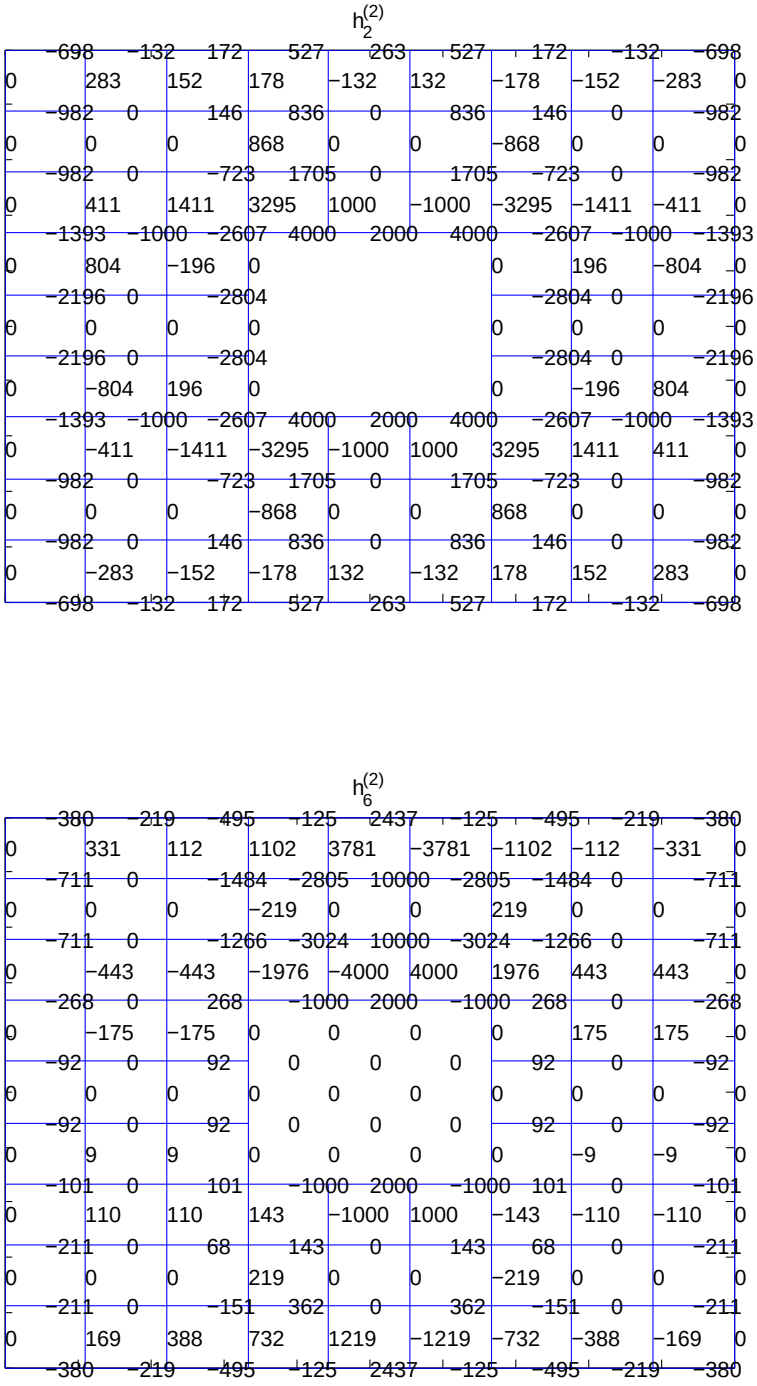

Figure 6.1: values of $h_2^{(2)}$ and values of $h_6^{(2)}$

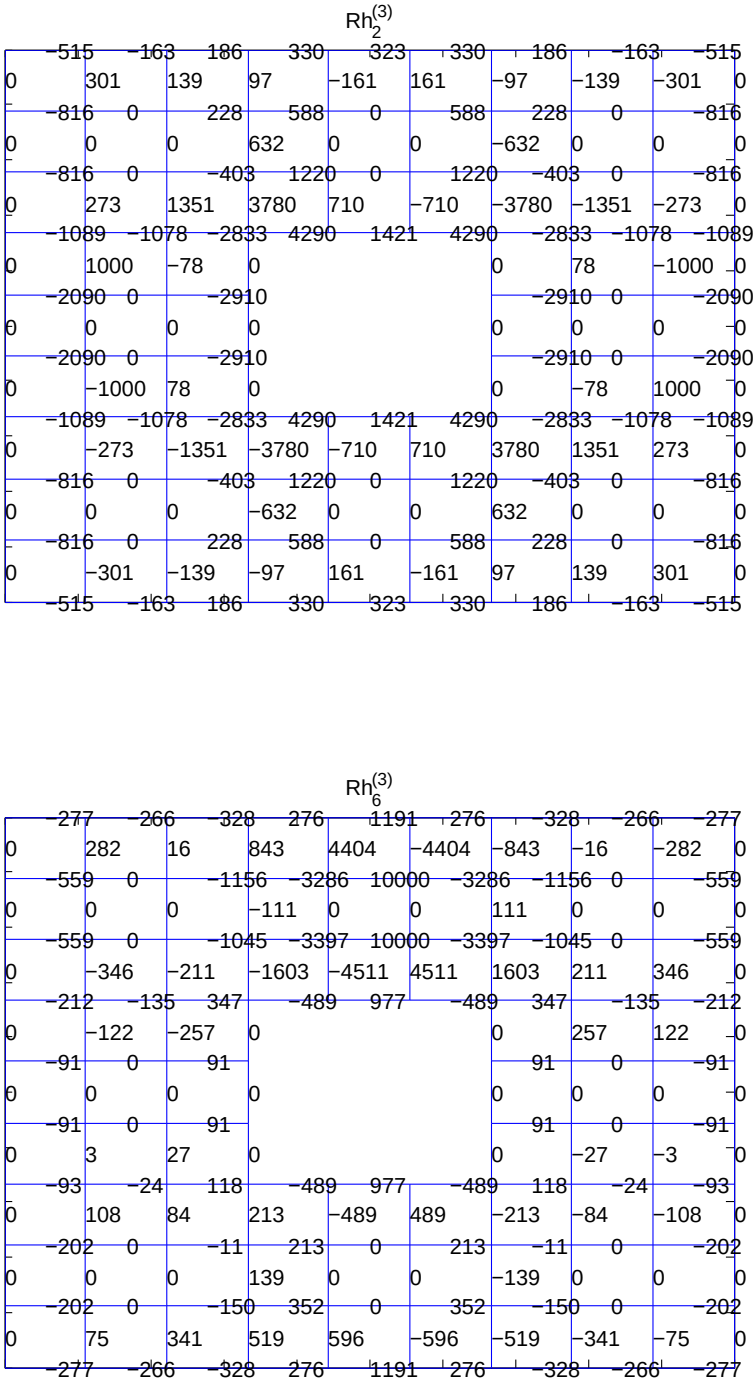

Figure 6.2: the restriction of $Rh_2^{(3)}$ and $Rh_6^{(3)}$ to $\tilde{E}_1^{(1)}$ where γ_1 is the top and bottom horizontal line

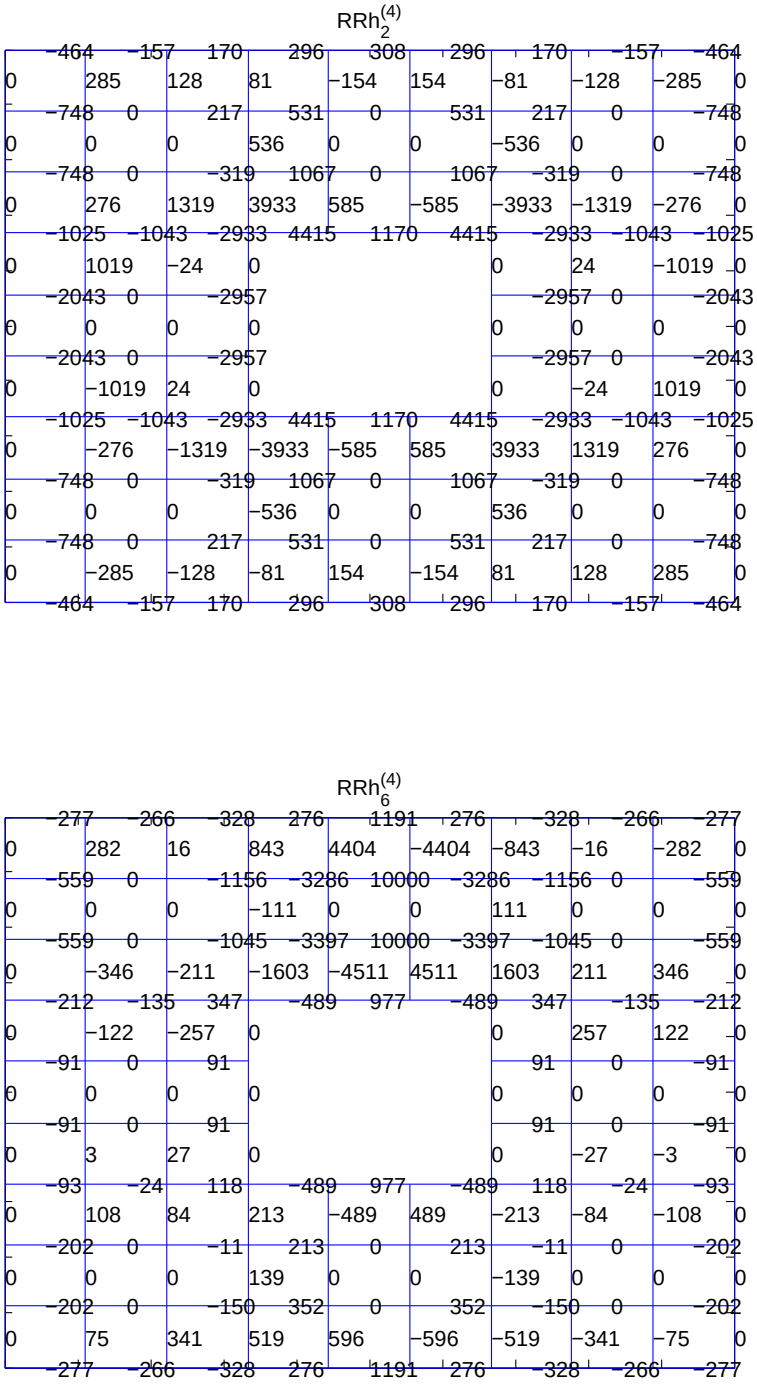

Figure 6.3: the restriction of $RRh_2^{(4)}$ and $RRh_6^{(4)}$ to $\tilde{E}_1^{(1)}$ where γ_1 is the top and bottom horizontal line

1k	$\|\|h^{(2)}_k - Rh^{(1)}_k\|\|$	$\|\|h^{(3)}_k - Rh^{(2)}_k\|\|$	$\|\|h^{(4)}_k - Rh^{(3)}_k\|\|$
1	0.1549	0.1476	0.1485
2	0.4647	0.1581	0.1349
3		0.2419	0.1452
4		0.2039	0.1468
5		0.2419	0.1452
6		0.2669	0.1458
7		0.2669	0.1458
8		0.2419	0.1452
9		0.2039	0.1468
10		0.2419	0.1452
11			0.2356
12			0.1953
13			0.1946
14			0.1950
15			0.1964
16			0.1950
17			0.1946
18			0.1953
19			0.2356
20			0.2639

Table 6.1: values of $\|h_k^{(m)} - Rh_k^{(m)}\|_2$

#of Eigenvalue / # of lines	1	2	3	4	5	6	7	8	9	10
1	1.0000	0.3321	0.4937	0.0535	0.4937	0.4875	0.4875	0.4937	0.0535	0.4937
2	1.0000	0.3927	2.0000	0.0685	0.1742	2.0000	0.1448	2.0000	0.0685	0.1742
3	1.0000	0.6818	2.0000	0.1069	0.1264	2.0000	0.0843	2.0000	0.1069	0.1264
4	1.0000	2.0000	0.5027	0.5153	0.1453	0.5070	0.4404	0.5027	0.5153	0.1453
5	1.0000	1.0000	0.0922	2.0000	0.0497	0.0369	0.0369	0.0922	2.0000	0.0497
6	1.0000	1.0000	0.0497	2.0000	0.0922	0.0369	0.0369	0.0497	2.0000	0.0922
7	1.0000	2.0000	0.1453	0.5153	0.5027	0.4404	0.5070	0.1453	0.5153	0.5027
8	1.0000	0.6818	0.1264	0.1069	2.0000	0.0843	2.0000	0.1264	0.1069	2.0000
9	1.0000	0.3927	0.1742	0.0685	2.0000	0.1448	2.0000	0.1742	0.0685	2.0000
10	1.0000	0.3321	0.4937	0.0535	0.4937	0.4875	0.4875	0.4937	0.0535	0.4937

#of Eigenvalues / # of lines	1	2	3	4	5	6	7	8	9	10
1	1.0000	0.2769	0.3982	0.0396	0.3982	0.3879	0.3879	0.3982	0.0396	0.3982
2	1.0000	0.2864	0.6450	0.0407	0.2488	0.6335	0.2361	0.6450	0.0407	0.2488
3	1.0000	0.2864	0.7645	0.0417	0.2209	0.7604	0.2067	0.7645	0.0417	0.2209
4	1.0145	0.3701	2.0289	0.0522	0.1748	2.0328	0.1488	2.0289	0.0522	0.1748
5	1.0000	0.3477	1.0000	0.0535	0.1125	1.0000	0.0987	1.0000	0.0535	0.1125
6	1.0000	0.3477	1.0000	0.0599	0.1111	1.0000	0.0947	1.0000	0.0599	0.1111
7	1.0145	0.5811	2.0289	0.0972	0.1272	2.0328	0.0959	2.0289	0.0972	0.1272
8	1.0000	0.8094	0.7537	0.1645	0.1142	0.7322	0.1244	0.7537	0.1645	0.1142
9	1.0000	1.0154	0.6166	0.1788	0.1195	0.5577	0.1242	0.6166	0.1788	0.1195
10	1.1735	2.0000	0.4047	0.3799	0.1492	0.4299	0.3285	0.4047	0.3799	0.1492
11	1.0000	1.0000	0.1743	0.5790	0.0497	0.0845	0.0418	0.1743	0.5790	0.0497
12	1.0000	1.0000	0.1620	0.7406	0.0403	0.0739	0.0418	0.1620	0.7406	0.0403
13	1.0216	1.0648	0.0970	2.0006	0.0445	0.0508	0.0506	0.0970	2.0006	0.0445
14	1.0000	1.0000	0.0476	1.0000	0.0423	0.0237	0.0237	0.0476	1.0000	0.0423
15	1.0000	1.0000	0.0423	1.0000	0.0476	0.0237	0.0237	0.0423	1.0000	0.0476
16	1.0216	1.0648	0.0445	2.0006	0.0970	0.0506	0.0508	0.0445	2.0006	0.0970
17	1.0000	1.0000	0.0403	0.7406	0.1620	0.0418	0.0739	0.0403	0.7406	0.1620
18	1.0000	1.0000	0.0497	0.5790	0.1743	0.0418	0.0845	0.0497	0.5790	0.1743
19	1.1735	2.0000	0.1492	0.3799	0.4047	0.3285	0.4299	0.1492	0.3799	0.4047
20	1.0000	1.0154	0.1195	0.1788	0.6166	0.1242	0.5577	0.1195	0.1788	0.6166
21	1.0000	0.8094	0.1142	0.1645	0.7537	0.1244	0.7322	0.1142	0.1645	0.7537
22	1.0145	0.5811	0.1272	0.0972	2.0289	0.0959	2.0328	0.1272	0.0972	2.0289
23	1.0000	0.3477	0.1111	0.0599	1.0000	0.0947	1.0000	0.1111	0.0599	1.0000
24	1.0000	0.3477	0.1125	0.0535	1.0000	0.0987	1.0000	0.1125	0.0535	1.0000
25	1.0145	0.3701	0.1748	0.0522	2.0289	0.1488	2.0328	0.1748	0.0522	2.0289
26	1.0000	0.2864	0.2209	0.0417	0.7645	0.2067	0.7604	0.2209	0.0417	0.7645
27	1.0000	0.2864	0.2488	0.0407	0.6450	0.2361	0.6335	0.2488	0.0407	0.6450
28	1.0000	0.2769	0.3982	0.0396	0.3982	0.3879	0.3879	0.3982	0.0396	0.3982

variation mc harmonic 1 forms.pdf

Table 6.2: Total variation of MC harmonic one forms along horizontal lines at level 2 and level 3

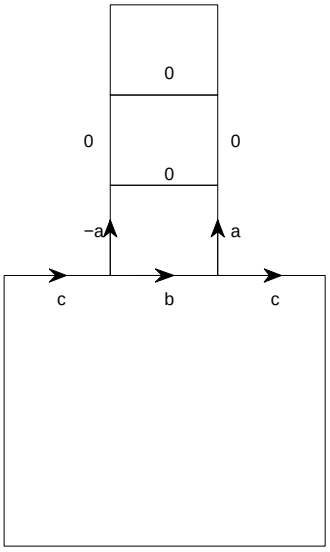

Figure 6.4:

Laplacians $-\tilde{\Delta}_0^{(m)}$ and $-\tilde{\Delta}_2^{(m)}$.

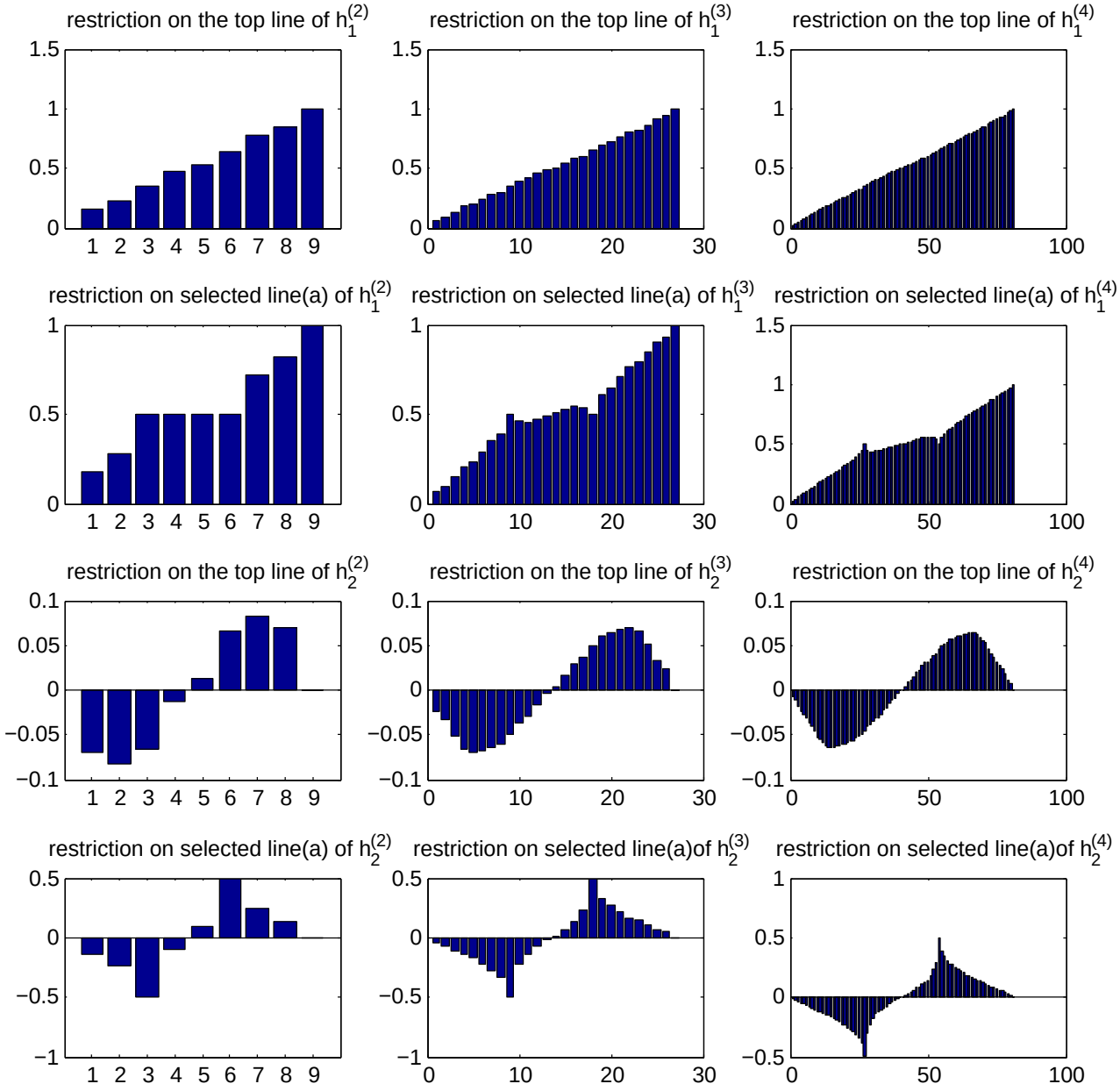

Figure 6.5: restrictions of some$h_k^{(m)}$

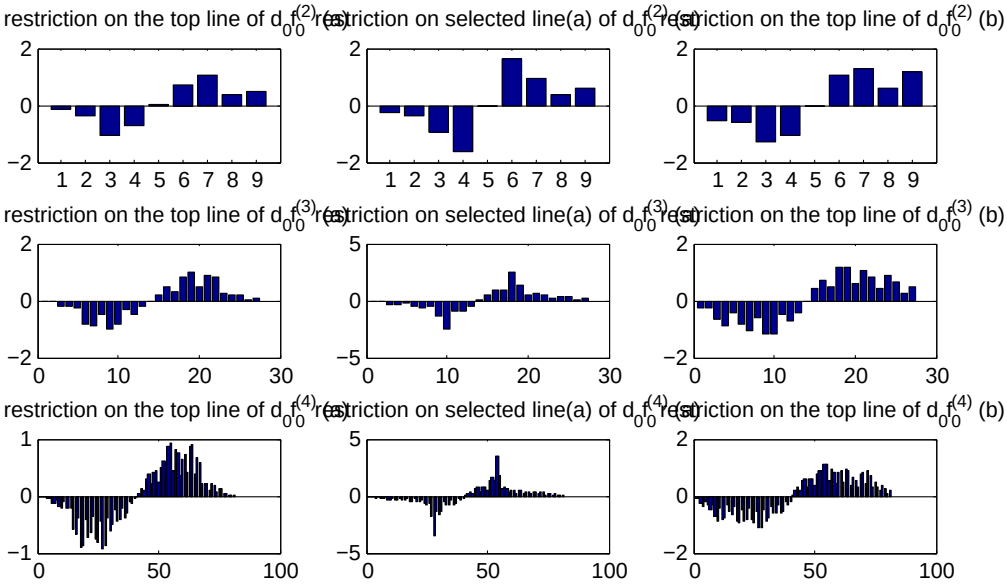

Figure 6.6: restrictions of some $-\tilde{\Delta}_0^{(m)}$

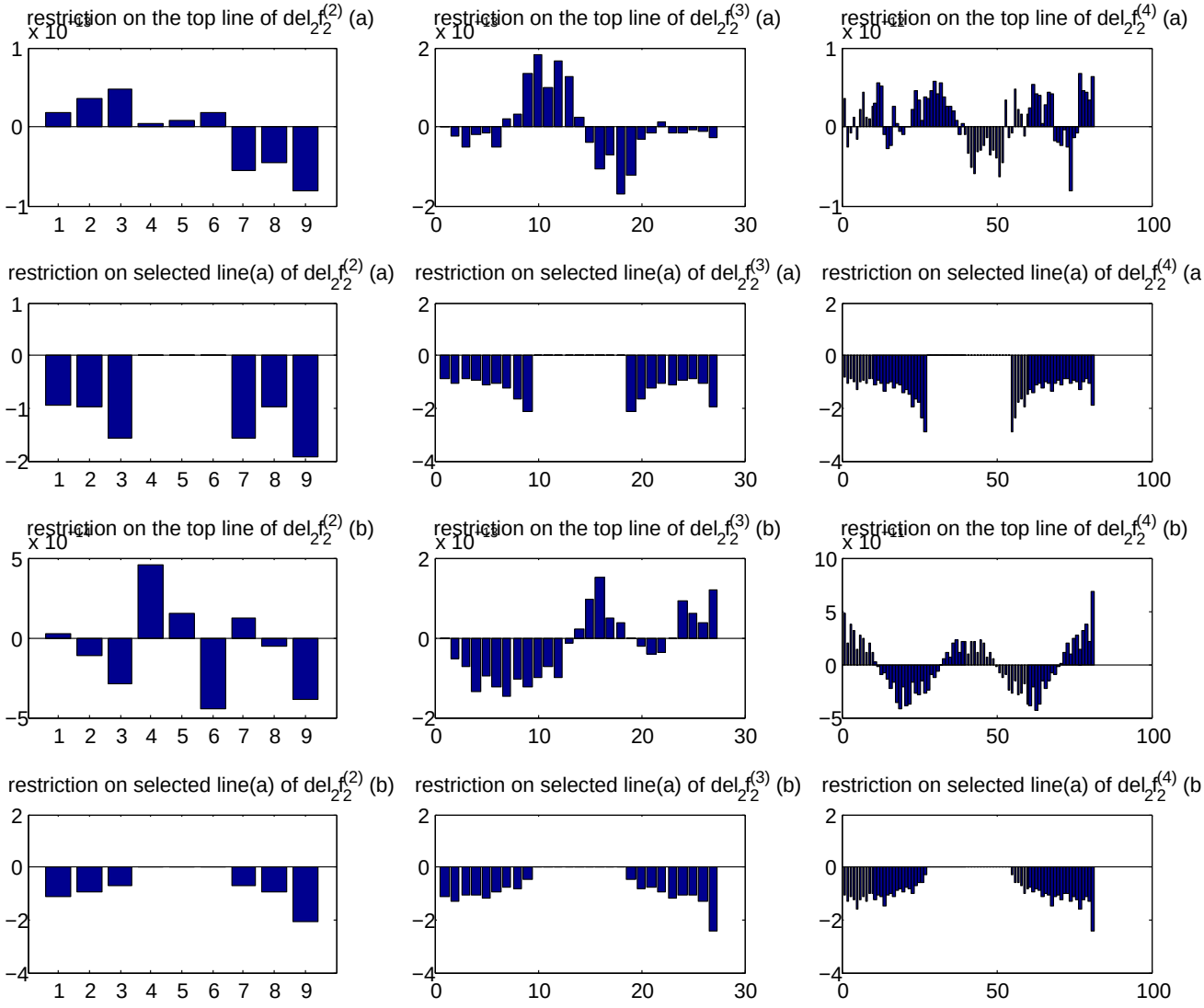

Figure 6.7: restrictions of some $-\tilde{\Delta}_2^{(m)}$

References

[1] [ACSY] Skye Arron, Zach Conn, Robert Strichartz, and Hui Yu, *Hodge-deRham Theory on Fractal Graphs and Fractals.*

[2] [ADS] T.Aougab, C.Y. Dong, and R.Strichartz,*Laplacians on a family of Julia sets II*, submitted for publication

[3] [BB1] M. Barlow and R. Bass,*On the resistance of the sierpinski carpet,* Proc. R. Soc. Lond. A(1990) **431** 345-360

[4] [BB2] M. Barlow, R.F. Bass, *coupling and Harnack inequalities for Sierpinski carpets,* Bull. Amer. Math. Soc., **29**(1993) 208-212

[5] [BBKT] M.T. Barlow, R.F. Bass, T. Kumagai, and A. Teplyaev, *Uniqueness of Brownian motion on Sierpinski carpets*. J. Eur. Math. Soc. (JEMS) **12** (2010), 655701.

[6] [BHS] Tyrus Berry, Steven Heilman, and Robert S. Strichartz, *outer Approximation of the Spectum of a Fractal Laplacian,* Experimental Mathematics, **18**, no. 4 (2009) 449-480

[7] [BKS] Matthew Begue, Tristan Kalloiatis and Robert Strichartz, *Harmonic functions and the spectrum of the Laplacian on the Sierpinski carpet*.

[8] [C] F. Cipriani. Diriclet forms on noncommutative spaces, L.N.M. 'Quantum Potential Thoery', 1954, U. Franz-M Schurmann eds. Springer-Verlag, New York, 2008, 161-172.

[9] [CGIS1] F. Cipriani, D Guido, T. Isola, and J. Sauvageot. Spectral triples on the Sierpinski gasket, AMS Meeting 'Analysis, Probability and Mathematical Physics on Fractals', Cornell U., 2011.

[10] [CGIS2] F. Cipriani, D Guido, T. Isola, and J. Sauvageot. Differential 1-forms, their integral and potential theory on the Sierpinski gasket, arXiv: 1105. 1995.

[11] [CS] F. Cipriani, and J. Sauvageot. Derivations as square roots of Dirichlet forms, J. Funct. Ana., 201 (2003), 78-120.

[12] [GI1] D Guido, T. Isola. Singular traces on semi-finite von Neumann algebras, J. Funct. Ana. 134 (1995), 451-485.

[13] [GI2] D Guido, T. Isol. Dimensions and singular traces for spectral triples, with applications to fractals, J. Funct. Anal. 203(2003) 362-400.

[14] [GI3] D Guido, T. Isola. Dimensions and singular traces for spectral triples for fractals in R^N, Advances in Operator Algebras and Mathematical Physics; Proceedings of the Conferene held in Sinaia, Romania, June 2003, F. Boca, O. Bratteli, R. Longo, H. Siedentop Eds., Theta Series in Advanced Mathematics, Bucharest 2005.

[15] [H] M. Hinz. Limit chains on the Sierpinski gasket, Indiana U. Math. J., to appear.

[16] [HS] Steven Heilman and Robert S. Strichartz, *Homotopies of Eigenfunctions and the Spectrum of the Laplacian on the Sierpinski Carpet*, Fractals **18** (2010), no.1, 1-34

[17] [IRT] M. Ionescu, L. G. Rogers, A. Teplyaev. Derivations and Dirichlet forms on fractals, arXiv: 1106. 1450.

[18] [Ki] Jun Kigami, *Analysis on fractals*, Cambridge Tracts in Mathematics, vol. 143, Cambridge University Press, Cambridge 2001.

[19] [KZ] S. Kusuoka and X. Y. Zhou, *Dirichlet form on fractals: Poincare constant and resistance*. Probab. Theory Related Fields **93** (2003), 169-196.

[20] [S3] Robert Strichartz, *Differential equations on fractals: a tutorial*, Princeton University Press, 2006.

[21] [W] www.math.cornell.edu/$yl\tilde{5}34$